

This is the accepted manuscript made available via CHORUS. The article has been published as:

Adaptation of the projector-augmented-wave formalism to the treatment of orbital-dependent exchange-correlation functionals

Xiao Xu and N A. W. Holzwarth

Phys. Rev. B **84**, 155113 — Published 14 October 2011

DOI: [10.1103/PhysRevB.84.155113](https://doi.org/10.1103/PhysRevB.84.155113)

Adaptation of the Projector Augmented Wave (PAW) formalism to the treatment of orbital-dependent exchange-correlation functionals

Xiao Xu and N. A. W. Holzwarth*

Department of Physics, Wake Forest University, Winston-Salem, North Carolina 27109, USA

(Dated: September 21, 2011)

This paper presents the formulation and numerical implementation of a self-consistent treatment of orbital-dependent exchange-correlation functionals within the Projector Augmented Wave (PAW) method of Blöchl [Phys. Rev. B **50** 17953 (1994)] for electronic structure calculations. The methodology is illustrated with binding energy curves for C in the diamond structure and LiF in the rock salt structure, comparing results from the Hartree-Fock (HF) formalism and the Optimized Effective Potential (OEP) formalism in the so-called KLI approximation [Krieger, Li, and Iafrate, Phys. Rev. A **45**, 101 (1992)] with those of the local density approximation (LDA). While the work here uses pure Fock exchange only, the formalism can be extended to treat orbital-dependent functionals more generally.

I. INTRODUCTION

In order to improve the physical representation of materials beyond that of conventional density functional theory,^{1,2} there has recently been renewed interest in the use of orbital-dependent exchange-correlation functionals including the use of hybrid functionals^{3–12} and the use of a combination of exact-exchange and random-phase approximation (EXX/RPA).^{13–19} At the moment, some of these treatments are treated non-self-consistently in the sense that the orbital-dependent contributions are treated by “post-processing” wavefunctions obtained from traditional density-dependent functionals. Because the orbital-dependent functionals are typically formulated in terms of integrals of the orbitals, the refinement of these treatments to full self-consistency requires updating the electron orbitals by solving integral-differential equations, a process which is, in principle, outside the realm of Kohn-Sham theory.

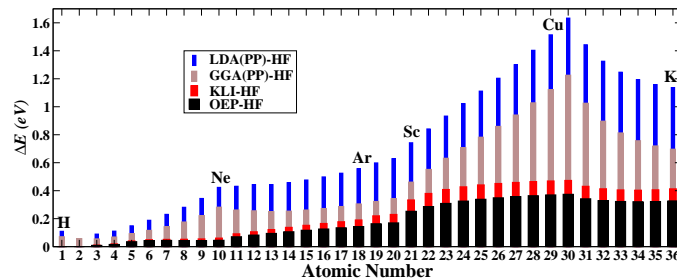


FIG. 1. (Color on line) Plot of total energy differences ΔE for spin unpolarized spherical atoms in their ground state configurations for $Z=1$ (H) through $Z=36$ (Kr), using the self-consistent Hartree-Fock energy as the reference. Results for ΔE obtained using self-consistent OEP or KLI calculations are compared with results obtained using self-consistent GGA or LDA wavefunctions to “post-process” the Fock exchange energies.

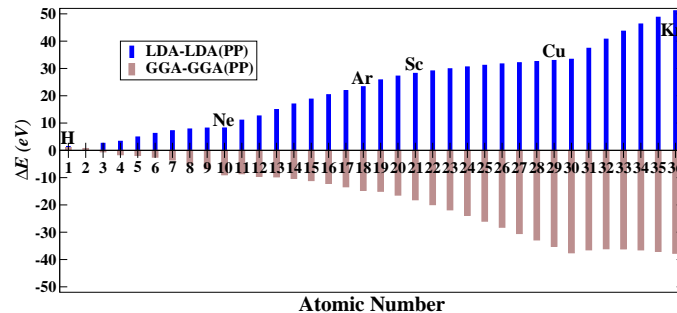


FIG. 2. (Color on line) Plot of energy differences ΔE for spin unpolarized spherical atoms in their ground state configurations using LDA or GGA exchange correlation functionals, each referenced to the corresponding energies obtained using the same wavefunctions to “post-process” the Fock exchange contribution.

In order to treat orbital-dependent contributions self-consistently within Kohn-Sham theory, it is necessary to represent its effects in terms of a local potential function known as an optimized effective potential (OEP).^{20–22} An interesting measure of the numerical effects of the various approaches, can be seen from the ground state energies of spin-unpolarized spherical atoms for the case of pure Fock exchange. Using ideas in the literature,^{23–28} we have modified our atomic code²⁹ in order to construct Figs. 1 and 2 and Table I. Figure 1 shows the results of calculating the ground state total energies of spin-unpolarized spherical atoms using the exact OEP approach, an approximate OEP approach (“KLI” described below) and the non-self-consistent post-processing result using LDA or GGA orbitals. In this figure, energy differences relative to Hartree-Fock are presented. Because of the variational properties of the Hartree-Fock solutions, all of the energy differences are positive.^{26,27} The “OEP-HF” results presented in Fig. 1 are consistent with results found earlier by Talman.²⁷ Also shown in Fig. 1 are the corresponding results generated by the approximation to OEP introduced by Kreiger, Li, and Iafrate (KLI).³⁰ The corresponding “KLI-HF” energies are slightly larger than the “OEP-HF”, differing by at most 0.1 eV for the 3d transition metals. Other approximate OEP methods have been developed, including the localized Hartree-Fock method,³¹ the common energy denominator,³² and the effective local potential³³ approximations. Bulat and Levy³⁴ have recently shown these methods to be equivalent to calculating the optimized effective potential within the subspace of occupied orbitals ($v^{\text{occ}}(\mathbf{r})$). We have evaluated $v^{\text{occ}}(r)$ for the spherical atoms in Fig. 1, finding the corresponding ground state energies to differ by at most 0.005 eV from those calculated within the KLI scheme.

By contrast to the self-consistent results, the results obtained by using wavefunctions from self-consistent GGA³⁵ or LDA³⁶ functionals and a post-processing evaluation of the Fock exchange, have significantly larger values of ΔE . On the one hand,

given that the self-consistent Hartree-Fock wavefunctions²⁸ are very similar in shape to those obtained from self-consistent LDA or GGA calculations, the large values of post processing energy differences shown in Fig. 1 is somewhat surprising. On the other hand, the Hartree-Fock post processing energies LDA(PP) and GGA(PP) themselves are considerably different from the self-consistent ground state LDA and GGA atomic energies as shown in Fig. 2. Interestingly, the plot of Fig. 2 shows that the LDA energy differences (LDA-LDA(PP)) have the opposite sign from the GGA energy differences (GGA-GGA(PP)), presumably due to the different correlation functional forms of LDA and GGA. The results of Figs. 1 and 2 suggest that post processing treatments may introduce unintended effects into the calculations. It is reasonable to expect that a self-consistent treatment will produce much more reliable results, benefiting from the power of the variational principle.

In order to have a more precise measure of the energy relationships, some representative total energies (for rare-gas atoms) are listed in Table I. Also listed in the table are literature results^{21,37} which are essentially identical to those generated with our code.

TABLE I. Total energies (in Ry) for some of the atoms shown in Figs. 1 and 2, comparing the self-consistent Hartree-Fock (HF), optimized effect potential (OEP), Kreiger-Li-Iafrate approximation (KLI), and occupied subspace (OCC) approximations with the post-processing energies calculated with local density approximation (LDA(PP)) and generalized gradient approximation (GGA(PP)) wavefunctions with the Fock exchange expression replacing the exchange-correlation contributions. Also listed are literature values for the HF, OEP, and KLI results.

	He	Ne	Ar	Kr
HF (this work)	-5.7234	-257.0942	-1053.6350	-5504.1100
HF (literature) ^a	-5.7234	-257.0942	-1053.6350	-5504.1100
OEP (this work)	-5.7234	-257.0908	-1053.6244	-5504.0859
OEP (literature) ^b	-5.7234	-257.0908	-1053.6244	-5504.0860
KLI (this work)	-5.7234	-257.0897	-1053.6210	-5504.0796
KLI (literature) ^b	-5.7234	-257.0896	-1053.6210	-5504.0796
OCC (this work)	-5.7234	-257.0896	-1053.6211	-5504.0793
LDA(PP) (this work)	-5.7191	-257.0630	-1053.5940	-5504.0264
GGA(PP) (this work)	-5.7191	-257.0734	-1053.6125	-5504.0587

^a Ref. 37.

^b Ref. 21.

These results for atoms provide a motivation for developing methods to calculate the orbital dependent terms accurately and self-consistently in extended systems. In previous work,²⁸ we showed how to formulate the Hartree-Fock theory within the projector augmented wave (PAW) formalism of Blöchl.³⁸ In this paper we extend this analysis to the OEP theory. For reasons discussed in Sec. II C, it turns out that treating the full OEP equations within the PAW formalism is computationally demanding. As a step close to reaching that goal, the present work focuses on the KLI approximation and its relationship with Hartree-Fock theory. It is assumed here that the orbital dependent contribution is that of the full Fock exchange. More importantly, extension of this approach to other orbital dependent functionals, including hybrid functionals and to random phase approximation treatments is expected to follow similar steps.

The outline of the paper is as follows. In Sec. II, we present the KLI formalism for spherical atoms, briefly reviewing the all-electron formulas³⁰ and discussing the frozen-orbital approximation. In Sec. II C we present the PAW formalism for spherical atoms and derive the relations for constructing basis and projector functions for a PAW-KLI treatment. More details of this work are presented in the Ph. D. Thesis of Xiao Xu.³⁹ In Sec. III we generalize the atomic formulations of both the Hartree-Fock and KLI approaches to treat periodic solids in a plane wave representation. The methods are demonstrated in terms of binding energy curves for diamond and for LiF in Sec. IV. Summary and conclusions are presented in Sec. V, where we also compare the PAW-HF and PAW-KLI approaches with previous treatments of Fock exchange reported in the literature. In particular, we note that a recent description of the *GP*AW code¹² which implements the PAW formalism on a real-space grid includes some PAW-HF formulations as well.

II. ELECTRONIC STRUCTURE OF SPHERICAL ATOMS WITHIN THE KLI APPROXIMATION

A. All-electron formalism

For simplicity, we discuss the formalism for spin-unpolarized, spherically averaged atoms and use the the same notation as in our previous work on developing a PAW formalism for Hartree-Fock theory.²⁸ The total electron energy takes the same functional form as in Hartree-Fock theory, as a sum of kinetic energy (E_K), nuclear energy (E_N), electron-electron or Hartree energy (E_H), and exchange energy (E_x):

$$E_{\text{tot}} = E_K + E_N + E_H + E_x. \quad (1)$$

Here the exchange energy is written in terms of radial integrals defined by Condon and Shortley⁴⁰

$$E_x = - \sum_{pq} \sum_{L=|l_p-l_q|}^{l_p+l_q} \frac{1}{2} \Theta_{pq}^L R_{pq;qp}^L, \quad (2)$$

where

$$R_{pq;st}^L \equiv e^2 \int \int dr dr' \frac{r_{\leq}^L}{r_{>}^{L+1}} \psi_p(r) \psi_q(r) \psi_s(r') \psi_t(r'). \quad (3)$$

Here the Fock weight factor Θ_{pq}^L for the moment L for the spherically averaged atom was derived by Ref. 23–25 and is given in Eq. (14) of Ref. 28. In contrast to Hartree-Fock theory, in the OEP approach, the one-electron orbitals $\{\psi_p(r)\}$ which appear in the energy expression are eigenstates of an effective Hamiltonian of the form

$$\mathcal{H} = \mathcal{K} + V_N(r) + V_H(r) + V_x(r) \quad \text{with} \quad \mathcal{H}\psi_p(r) = \epsilon_p \psi_p(r). \quad (4)$$

Here the expressions for the nuclear and Hartree potentials are identical to those of Ref. 28. In the full OEP theory, the local potential $V_x(r)$ can be determined iteratively in terms of orbital shift functions⁴¹ $g_p(r)$ which are solutions to inhomogeneous differential equations of the form:

$$(\mathcal{H} - \epsilon_p) g_p(r) = X_p(r) - V_x(r) \psi_p(r) - (\bar{U}_{x\,p} - \bar{V}_{x\,p}) \psi_p(r), \quad (5)$$

where

$$\bar{V}_{x\,p} \equiv \langle \Psi_p | V_x | \Psi_p \rangle \quad \text{and} \quad \bar{U}_{x\,p} \equiv \langle \Psi_p | X_p \rangle. \quad (6)$$

The exchange integral function $X_p(r)$ is identical to that defined in Eq. (19) of Ref. 28 except that the orbitals $\{\psi_p(r)\}$ are the self-consistent OEP orbitals instead of the self-consistent Hartree-Fock orbitals. It takes the form

$$X_p(r) = - \sum_q \sum_{L=|l_p-l_q|}^{l_p+l_q} \frac{1}{N_p} \Theta_{pq}^L W_{qp}^L(r) \psi_q(r), \quad (7)$$

where

$$W_{qp}^L(r) \equiv e^2 \int dr' \frac{r_{\leq}^L}{r_{>}^{L+1}} \psi_q(r') \psi_p(r'). \quad (8)$$

For the full OEP treatment, the converged local exchange potential $V_x(r)$ is obtained when the combined shift function vanishes:^{26,41–43}

$$\sum_p N_p g_p(r) \psi_p(r) = 0. \quad (9)$$

The Krieger, Li, and Iafrate (KLI) approximation³⁰ to the OEP is based on the reasonable assumption that the orbital shift functions $g_p(r)$ are numerically small so that the left hand side of Eq. (5) can be set to 0.⁴⁴ Then a local exchange potential function $V_x^{\text{KLI}}(r)$ can be found which satisfies the following KLI equation.

$$\begin{aligned} V_x^{\text{KLI}}(r) n(r) &= \sum_p N_p \psi_p(r) X_p^{\text{KLI}}(r) \\ &+ \sum_p N_p |\psi_p(r)|^2 (\bar{V}_{x\,p}^{\text{KLI}} - \bar{U}_{x\,p}^{\text{KLI}}) \end{aligned} \quad (10)$$

The radial density function is defined

$$n(r) \equiv \sum_p N_p |\psi_p(r)|^2. \quad (11)$$

In order to solve Eq. (10) it is first necessary to determine the matrix elements $\bar{V}_{x\,p}^{\text{KLI}}$. The p index references each of the S atomic shells. The boundary conditions require that for the shell $p \equiv o$ corresponding to the outer most orbital $\psi_o(r)$, the exchange potential matrix element must satisfy^{21,30}

$$\bar{V}_{x\,o}^{\text{KLI}} \equiv \bar{U}_{x\,o}^{\text{KLI}}. \quad (12)$$

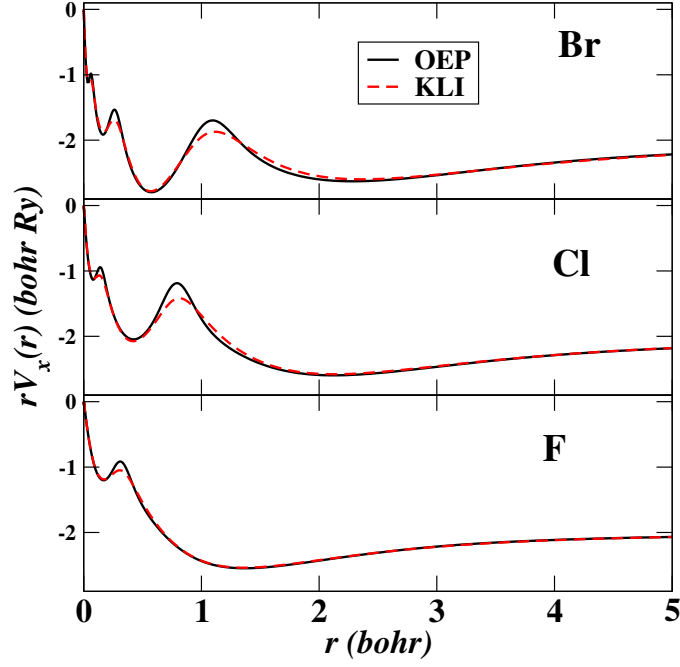


FIG. 3. (Color on line) Comparison of OEP and KLI functions of $V_x(r)$ for Br, Cl, and F in their ground states.

For the $S - 1$ shell indices $p \neq o$, the following linear equations must be satisfied:^{21,30}

$$\sum_{q \neq o} [\delta_{pq} - \Gamma_{pq} N_q] \Delta_q = \Xi_p - \bar{U}_{xp}^{\text{KLI}}, \quad (13)$$

where

$$\Delta_q \equiv \bar{V}_{xq}^{\text{KLI}} - \bar{U}_{xq}^{\text{KLI}}. \quad (14)$$

Here

$$\Gamma_{pq} \equiv \int dr \frac{|\psi_p(r)|^2 |\psi_q(r)|^2}{n(r)}, \quad (15)$$

and

$$\Xi_p \equiv \int dr \frac{|\psi_p(r)|^2 \sum_q N_q \psi_q(r) X_q^{\text{KLI}}(r)}{n(r)}. \quad (16)$$

Once the matrix elements $\bar{V}_{xp}^{\text{KLI}}$ are determined from Eqs. (12, 13, and 14), the KLI exchange potential $V_x^{\text{KLI}}(r)$ can be determined from Eq. (10). Figure 3 shows 3 examples of $V_x^{\text{KLI}}(r)$ in comparison with corresponding local potentials calculated using the full OEP formalism. The small differences in the potentials shown here is consistent with results on other materials presented in the original KLI manuscript.³⁰

B. Frozen core orbital approximation

The arguments favoring the frozencore *orbital* treatment over the frozencore *potential* treatment for the Hartree-Fock formalism were presented in our previous work²⁸ and apply to the KLI formalism as well. The frozencore orbital approximation within the KLI approach is almost a trivial extension of the all-electron treatment. The equations have the same form as given above, with the summation over shells p including both valence states $\Psi_v(\mathbf{r})$ which are updated and core states $\Psi_c(\mathbf{r})$ which are “frozen” to the reference configuration form.⁴⁵ We note that in order that the KLI exchange potential (10) remain orbital independent and especially independent of core-valence orbital labels, it is essential for both valence and (frozen) core contributions

be included in the evaluation of Eq. (10). As we will see, this will be true in the PAW formulation as well. On the other hand, it is often convenient to remove the constant contributions to the energy, and to define a valence electron energy from terms that involve valence electrons alone and terms that involve interactions between core and valence electrons:

$$E_{\text{val}} = E_K^v + E_N^v + E_H^{cv} + E_H^{vv} + E_x^{cv} + E_x^{vv}. \quad (17)$$

Numerical results for the frozen core orbital approximation of KLI are comparable to those of the frozen core orbital approximation of Hartree-Fock reported in our earlier work.²⁸ For example, we considered ionization energies for spherically averaged $3d$ atoms. The results are shown in Fig. 4 comparing the Hartree-Fock and KLI results with those obtained using the local density approximation (LDA).³⁶ The Hartree-Fock and KLI ionization energies are very similar throughout the $3d$ series, differing from each other by less than 0.08 eV. Not surprisingly, the LDA ionization energies differ from the HF ionization energies by roughly 2 eV. Using the core states defined by the configuration of Ar, the errors introduced by calculating the ionization energies within frozencore approximations are not visible on this scale. For the frozencore orbital approach within HF, KLI, and LDA formalisms, the average error in the ionization energies is 0.002 eV, 0.002 eV, and 0.001 eV respectively. We also calculated the ionization energies using the frozen core potential approach described in Ref.²⁸ (labeled HFV) on the graph). In this frozencore potential approach, the average error in calculating the ionization energies is 0.05 eV, 25 times larger than that of the frozencore orbital approach. This motivates the adoption of a frozencore orbital treatment for our PAW formulation, which can be accomplished in a straightforward way.

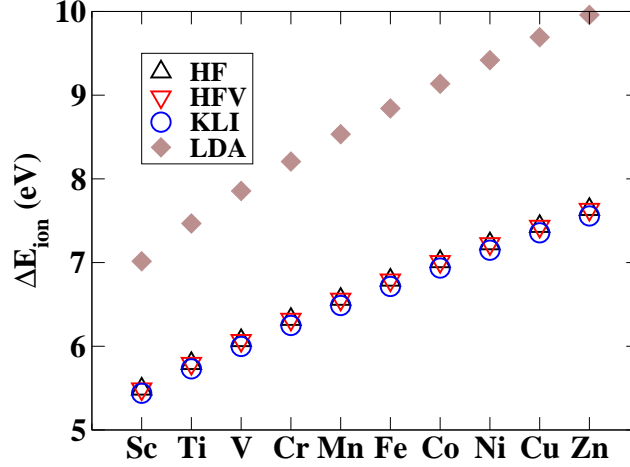


FIG. 4. (Color on line) Plot of ionization energies for spherically averaged $3d$ atoms, assuming transitions $3d^x 4s^2 \rightarrow 3d^x 4s^1$, using the HF, KLI, and LDA exchange approximations. The results designated as HFV were calculated using the frozencore potential approximation as described in Ref. 28.

C. PAW formalism for a spherical atom

1. Motivation for various approximations

In addition to the approximations associated with the PAW formalism itself, the treatment presented here uses two major approximations which need justification. We first consider the reason for using the KLI approximation rather than directly solving the full OEP equations. The reason follows from the fact that the PAW formalism is designed to represent a valence electron wavefunction $\Psi_v(\mathbf{r})$ in the form

$$\Psi_v(\mathbf{r}) = \tilde{\Psi}_v(\mathbf{r}) + \sum_{ai} \left(\Phi_i^a(\mathbf{r} - \mathbf{R}^a) - \tilde{\Phi}_i^a(\mathbf{r} - \mathbf{R}^a) \right) \langle \tilde{P}_i^a | \tilde{\Psi}_v \rangle, \quad (18)$$

where a denotes an atomic site (which is trivial for a spherical atom) and i denotes atom-centered functions which include $|\Phi_i^a\rangle$, $|\tilde{\Phi}_i^a\rangle$, and $|\tilde{P}_i^a\rangle$ for the all-electron basis functions, pseudo basis functions, and projector functions respectively. Typically, the index i represents a small number of states (one or two states per angular momentum channel) to represent the electron wavefunction in typical environments found in solids. In order to adapt the PAW formalism to the OEP treatment, it is necessary

to use this form to also represent the orbital shift function $g_v(r)$ defined in Eq. (5). Because of the oscillatory shape of these $g_v(r)$ functions, it is necessary to significantly increase the number of one-center basis functions included in the general transformation of Eq. (18). The recent paper by Bulat and Levy³⁴ clarified this point by showing that the full optimized effective potential function can be determined as a sum of contributions from the space of occupied orbitals to determine $v_x^{\text{occ}}(\mathbf{r})$ plus additional terms generated by all unoccupied states. These additional terms require additional basis functions. While the use of additional basis functions in the PAW expansion is in principle possible, it is computationally expensive. Some details are presented in the Appendix (A). In fact, recent work by Harl and co-workers¹⁸ describes the use of these additional basis functions for a post-processing treatment of the random phase approximation within the PAW formalism. In this case, the additional basis functions are physically motivated by the excited state contributions to the random phase formalism, while in the exchange-only OEP treatment they are needed only to fulfill the numerical requirements of the equations which represent only the ground state of the system. On the other hand, the minimal basis PAW formalism is well-suited to represent the approximate OEP equations in the KLI approach accurately and efficiently. The PAW-KLI approach presented here can be also extended to the full occupied space approximation $v_x^{\text{occ}}(\mathbf{r})$ with few changes to the formalism.

The second approximation in this work is made for simplicity. We have argued that the core states provide important contributions to the exchange interactions and in Ref. 28 we have shown how to treat extended core states with frozen-core pseudo-wavefunctions $\tilde{\psi}_c(r)$ and their fully nodal counterparts $\psi_c(r)$. While including these upper core wavefunctions in the calculation is straightforward, in order to simplify the presentation in the present work, we make the assumption that for all core wavefunctions $\psi_c(r) \equiv 0$. This can be made precise for any system, by treating upper core states as valence states (with additional computational cost), leaving the core designation to refer only to states whose orbitals are well-confined within the augmentation sphere. What this means is that the summations over all states in the pseudo-space includes only valence states. The core states then only enter the calculations through the one-center all-electron terms. The more general case of allowing for non-zero $\tilde{\psi}_c(r)$ for upper core wavefunctions can be derived by straightforward extension.

2. PAW-KLI formalism for atoms

The purpose of deriving the PAW-KLI equations of a spherical atom is to define the consistent basis and projector functions which satisfy the atomic PAW-KLI equations for the reference configuration and to provide the basis for extending the formalism to a more general system. The PAW representation of the radial electron density of a spherical atom takes the form^{28,38}

$$n(r) = \tilde{n}(r) + (n^a(\mathbf{r}) - \tilde{n}^a(r)), \quad (19)$$

where $\tilde{n}(r)$ represents the radial pseudodensity defined over all space and the terms with superscript a represent the atomic density confined within the augmentation sphere. For materials, the single index a will be replaced by a summation of one-center contributions over all augmentation spheres.

The PAW transformation allows us to approximate the left hand side of the of KLI equality – Eq. (10) – by the form

$$V_x^{\text{KLI}}(r) n(r) = \tilde{V}_x^{\text{KLI}}(r) \tilde{n}(r) + \left(V_x^{a\text{KLI}}(r) n^a(r) - \tilde{V}_x^{a\text{KLI}}(r) \tilde{n}^a(r) \right). \quad (20)$$

Here $\tilde{V}_x^{\text{KLI}}(r)$ denotes the smooth pseudo exchange potential in the KLI approximation which is defined over all space while $V_x^{a\text{KLI}}(r)$ and $\tilde{V}_x^{a\text{KLI}}(r)$ denote the atom-centered all-electron and pseudo exchange functions, respectively which will appear in atom-centered matrix elements in the PAW formalism. In order to determine these three contributions to the exchange potential, we assume that each of them satisfies Eq. (10) in their respective spacial and functional domains.

The pseudo-space contribution takes the form written

$$\begin{aligned} \tilde{V}_x^{\text{KLI}}(r) \tilde{n}(r) &= \sum_v N_v \tilde{\psi}_v(r) \tilde{X}_v^{\text{KLI}}(r) \\ &\quad + \sum_v N_v \left| \tilde{\psi}_v(r) \right|^2 (\bar{V}_{xv}^{\text{KLI}} - \bar{U}_{xv}^{\text{KLI}}). \end{aligned} \quad (21)$$

Within the augmentation region, the two types of one-center contributions can be written

$$\begin{aligned} V_x^{a\text{KLI}}(r) n^a(r) &= \sum_p N_p \psi_p^a(r) X_p^{a\text{KLI}}(r) \\ &\quad + \sum_p N_p \left| \psi_p^a(r) \right|^2 (\bar{V}_{xp}^{\text{KLI}} - \bar{U}_{xp}^{\text{KLI}}), \end{aligned} \quad (22)$$

and

$$\begin{aligned}\tilde{V}_x^{a\text{KLI}}(r) \tilde{n}^a(r) &= \sum_v N_v \tilde{\psi}_v^a(r) \tilde{X}_v^{a\text{KLI}}(r) \\ &+ \sum_v N_v \left| \tilde{\psi}_v^a(r) \right|^2 (\bar{V}_{xv}^{\text{KLI}} - \bar{U}_{xv}^{\text{KLI}}).\end{aligned}\quad (23)$$

The $\bar{V}_{xv}^{\text{KLI}}$ and $\bar{U}_{xv}^{\text{KLI}}$ matrix elements that appear in each of the three equations are determined from a sum of contributions in the form:

$$\begin{aligned}\bar{V}_{xp}^{\text{KLI}} &= \langle \tilde{\Psi}_p | \tilde{V}_x^{\text{KLI}} | \tilde{\Psi}_p \rangle + \\ &\left(\langle \Psi_p^a | V_x^{a\text{KLI}} | \Psi_p^a \rangle - \langle \tilde{\Psi}_p^a | \tilde{V}_x^{a\text{KLI}} | \tilde{\Psi}_p^a \rangle \right),\end{aligned}\quad (24)$$

and

$$\bar{U}_{xp}^{\text{KLI}} = \langle \tilde{\Psi}_p | \tilde{X}_p^{\text{KLI}} \rangle + \left(\langle \Psi_p^a | X_p^{a\text{KLI}} \rangle - \langle \tilde{\Psi}_p^a | \tilde{X}_p^{a\text{KLI}} \rangle \right).\quad (25)$$

In these expressions and in others in this section, the index p for core states is non-trivial only for the one-center all-electron terms.

In order to determine the unknown coefficients $\bar{V}_{xp}^{\text{KLI}}$, a set of linear equations similar to Eq. (13) must be solved. These can be written in the form

$$\sum_{q \neq o} [\delta_{pq} - \Gamma_{pq}^{\text{PAW}} N_q] \Delta_q = \Xi_p^{\text{PAW}} - \bar{U}_{xq}^{\text{KLI}}.\quad (26)$$

Once the unknown matrix elements Δ_q have been determined, they can be used in Eqs. (21, 22, and 23) to determine $\tilde{V}_x^{\text{KLI}}(r)$, $V_x^{a\text{KLI}}(r)$, and $\tilde{V}_x^{a\text{KLI}}(r)$, respectively. In Eq. (26) the Γ_{pq}^{PAW} matrix elements are given by

$$\begin{aligned}\Gamma_{pq}^{\text{PAW}} &= \int_0^\infty dr \frac{\left| \tilde{\psi}_p(r) \right|^2 \left| \tilde{\psi}_q(r) \right|^2}{\tilde{n}(r)} + \\ &\int_0^{r_c^a} dr \left[\frac{\left| \psi_p^a(r) \right|^2 \left| \psi_q^a(r) \right|^2}{n^a(r)} - \frac{\left| \tilde{\psi}_p^a(r) \right|^2 \left| \tilde{\psi}_q^a(r) \right|^2}{\tilde{n}^a(r)} \right].\end{aligned}\quad (27)$$

The exchange coefficients Ξ_p^{PAW} are given by

$$\begin{aligned}\Xi_p^{\text{PAW}} &= \int_0^\infty dr \frac{\left| \tilde{\psi}_p(r) \right|^2 \sum_q N_q \tilde{\psi}_q(r) \tilde{X}_q^{\text{KLI}}(r)}{\tilde{n}(r)} + \\ &\int_0^{r_c^a} dr \left[\frac{\left| \psi_p^a(r) \right|^2 \sum_q N_q \psi_q^a(r) X_q^{a\text{KLI}}(r)}{n^a(r)} \right. \\ &\quad \left. - \frac{\left| \tilde{\psi}_p^a(r) \right|^2 \sum_q N_q \tilde{\psi}_q^a(r) \tilde{X}_q^{a\text{KLI}}(r)}{\tilde{n}^a(r)} \right].\end{aligned}\quad (28)$$

In Eqs. (27 and 28), the one center integrands are confined within the augmentation spheres ($r \leq r_c^a$) and contributions for p or q representing core states come only from the one-center all-electron terms.

In these expressions the pseudo exchange kernel is given by

$$\tilde{X}_v^{\text{KLI}}(r) = - \sum_{v'} \sum_{L=|l_v-l_{v'}|}^{l_v+l_{v'}} \frac{1}{N_v} \Theta_{vv'}^L \tilde{W}_{v'v}^L(r) \tilde{\psi}_{v'}(r),\quad (29)$$

with the interaction function evaluated according to

$$\tilde{W}_{v'v}^L(r) = e^2 \int dr' \frac{r_{\leq}^L}{r_{>}^{L+1}} \left[\tilde{\psi}_{v'}(r') \tilde{\psi}_v(r') + \widehat{M}_{v'v}^L(r') \right].\quad (30)$$

The summation over shells v and v' includes contributions from valence pseudo-wavefunctions $\tilde{\psi}_v(r)$. The moment function $\tilde{M}_{v'v}^L(r)$ is defined by Eq. (58) of Ref. 28.

For the one-center all-electron terms (22), the sum over p includes both valence and core contributions. The one-center all-electron orbitals for the valence states are given by

$$\psi_v^a(r) = \sum_i \langle \tilde{P}_i^a | \tilde{\Psi}_v \rangle \phi_i^a(r). \quad (31)$$

The PAW functions are denoted by $p_i^a(r)$, $\phi_i^a(r)$, and $\tilde{\phi}_i^a(r)$ for the radial projector, all-electron basis, and pseudo basis functions, respectively, while the capitalized forms (for example $\tilde{P}_i^a(r)$) denote the corresponding full 3-dimensional function. For the all-electron core contributions ($p = c$), the all-electron frozen-core functions $\psi_c^a(r)$ are used directly. These expressions for the atom-centered radial wavefunctions are only valid in the augmentation region $0 \leq r \leq r_c^a$. Fortunately, in all the expressions in which they are used, it is only necessary to evaluate the one-center functions in the augmentation regions. For evaluating the one-center all-electron exchange kernel $X_p^{a\text{KLI}}(r)$ the following form for the interaction integrals can be used for $0 \leq r \leq r_c^a$

$$W_{qp}^{aL}(r) = \sum_{ij} \langle \tilde{\Psi}_q | \tilde{P}_i^a \rangle \langle P_j^a | \tilde{\Psi}_p \rangle w_{ij}^{aL}(r) + \left(\frac{r}{r_c^a} \right)^L \omega_{qp}^{aL}, \quad (32)$$

where

$$w_{ij}^{aL}(r) \equiv e^2 \int_0^{r_c^a} dr' \frac{r'^L}{r_{>}^{L+1}} \phi_i^a(r') \phi_j^a(r'). \quad (33)$$

This expression is correct for both shell indices q and p corresponding to valence states. If one or both of them correspond to core states, the expressions are modified according to

$$\langle \tilde{\Psi}_c^a | \tilde{P}_i^a \rangle \rightarrow \delta_{ci}, \quad (34)$$

and the replacement of ϕ_i^a with $\psi_c^a(r)$.

The one-center pseudo orbitals for the valence states are given by

$$\tilde{\psi}_v^a(r) = \sum_i \langle \tilde{P}_i^a | \tilde{\Psi}_v \rangle \tilde{\phi}_i^a(r), \quad (35)$$

using the same notation as above. For evaluating the one-center pseudo exchange kernel $\tilde{X}_v^{a\text{KLI}}(r)$, the following form for the interaction integral can be used for $0 \leq r \leq r_c^a$:

$$\tilde{W}_{v'v}^{aL}(r) = \sum_{ij} \langle \tilde{\Psi}_{v'} | \tilde{P}_i^a \rangle \langle P_j^a | \tilde{\Psi}_v \rangle \tilde{w}_{ij}^{aL}(r) + \left(\frac{r}{r_c^a} \right)^L \omega_{v'v}^{aL}, \quad (36)$$

where

$$\tilde{w}_{ij}^{aL}(r) \equiv e^2 \int_0^{r_c^a} dr' \frac{r'^L}{r_{>}^{L+1}} \left[\tilde{\phi}_i^a(r') \tilde{\phi}_j^a(r') + \hat{m}_{ij}^{aL}(r') \right], \quad (37)$$

where the augmentation moment $\hat{m}_{ij}^{aL}(r)$ has been defined in Eq. (53) of Ref. 28. For convenience we repeat the definition here:

$$\hat{m}_{ij}^{aL}(r) \equiv m_{ij}^{aL} g_L^a(r), \quad (38)$$

where the charge moment coefficient m_{ij}^{aL} is given in terms of the i and j basis functions

$$m_{ij}^{aL} \equiv \int_0^{r_c^a} dr r^L \left(\phi_i^a(r) \phi_j^a(r) - \tilde{\phi}_i^a(r) \tilde{\phi}_j^a(r) \right), \quad (39)$$

and the augmentation shape function $g_L^a(r)$ is localized to the augmentation sphere, $0 \leq r \leq r_c^a$ and is normalized according to

$$\int_0^{r_c^a} dr r^L g_L^a(r) = 1. \quad (40)$$

In the interaction integrals for valence states in Eqs. (32 and 36) the same constants $\omega_{v'v}^{aL}$ appear. (The corresponding contributions vanish for localized core states.) In atomic calculations, the constants can be evaluated from the pseudo-pair-density outside the augmentation region:

$$\omega_{v'v}^{aL} \equiv (r_c^a)^L \int_{r_c^a}^{\infty} dr' \frac{\tilde{\psi}_{v'}(r') \tilde{\psi}_v(r')}{r'^{L+1}}. \quad (41)$$

In general, it is necessary to evaluate the constants $\omega_{v'v}^{aL}$ within the augmentation region. This can be accomplished by matching the boundary values of $W_{v'v}^{aL}(r_c^a)$ and $\tilde{W}_{v'v}^{aL}(r_c^a)$ to that of $\tilde{W}_{v'v}^L(r_c^a)$, the full pseudo interaction integral given in Eq. (30).

In terms of the given representations of orbitals and of the interaction integrals, the one-center all-electron exchange kernel function can be written:

$$X_p^{a\text{KLI}}(r) = - \sum_q \sum_{L=|l_p-l_q|}^{l_p+l_q} \frac{1}{N_p} \Theta_{pq}^L W_{qp}^{aL}(r) \psi_q^a(r), \quad (42)$$

and the one-center pseudo exchange kernel function can be written:

$$\tilde{X}_v^{a\text{KLI}}(r) = - \sum_{v'} \sum_{L=|l_v-l_{v'}|}^{l_v+l_{v'}} \frac{1}{N_v} \Theta_{vv'}^L \tilde{W}_{v'v}^{aL}(r) \tilde{\psi}_{v'}^a(r). \quad (43)$$

The expressions for the exchange kernel functions given in Eqs. 30, 42, and 43 are consistent with the PAW exchange kernel function given in Ref. 28 for the Hartree-Fock formalism $X_v^{\text{PAW}}(\mathbf{r}) = \tilde{X}_v^{\text{HF}}(\mathbf{r}) + \sum_{ai} |\tilde{P}_i^a\rangle X_{iv}^{a\text{HF}}$, with the correspondence

$$\tilde{X}_v^{\text{HF}}(\mathbf{r}) \rightarrow \tilde{X}_v^{\text{KLI}}(r) \quad (44)$$

and the approximate relation

$$X_{iv}^{a\text{HF}} \approx \langle \Phi_i^a | X_v^{a\text{KLI}} \rangle - \langle \tilde{\Phi}_i^a | \tilde{X}_v^{a\text{KLI}} \rangle. \quad (45)$$

These approximate relationships rely on the fact that within the augmentation spheres, $\psi_v(r) \approx \psi_v^a(r)$, based on the PAW expansion given in Eq. (35) and approximate completeness relations³⁸ for $0 \leq r \leq r_c^a$ such as:

$$\sum_i |\tilde{P}_i^a\rangle \langle \tilde{\Phi}_i^a| \approx \delta(\mathbf{r} - \mathbf{r}') \quad (46)$$

for the the pseudospace functions.

The equations given above can be used to self-consistently solve the Kohn-Sham equations within the PAW-KLI approximation, given a PAW dataset of basis, projector, and pseudopotential functions. For the construction of a PAW dataset in the PAW-KLI approximation, it is necessary to evaluate these expressions for the reference configuration used to generate the basis and projector functions. In this case, Eqs. (21) and (23) are identical to each other, and Eq. (22) is identical to the all-electron result Eq. (10). By evaluating Eq. (21) or (23) to determine the pseudo exchange potential $\tilde{V}_x^a(r)$, for the given choice of basis and projector functions, it is possible to determine the unscreened local pseudopotential $\tilde{V}_{\text{loc}}^a(r)$ from the chosen screened pseudopotential $V^{a\text{PS}}(r)$ according to

$$\tilde{V}_{\text{loc}}^a(r) = V^{a\text{PS}}(r) - Z^a \hat{v}_0^a(r) - \tilde{V}_H^a(r) \Big|_{\text{ref}} - \tilde{V}_x^a(r) \Big|_{\text{ref}}. \quad (47)$$

Here $\hat{v}_0^a(r)$ is defined as the Coulomb potential associated with the $L = 0$ augmentation shape function $g_L^a(r)$. The Hartree contribution can be evaluated as a sum of core and valence contributions in the form

$$\tilde{V}_H^{a\text{c}}(r) \equiv Q_{\text{core}}^a \hat{v}_0^a(r) \text{ and } \tilde{V}_H^{av}(r) \Big|_{\text{ref}} \equiv \sum_v N_v \tilde{W}_{vv}^0(r) \Big|_{\text{ref}}. \quad (48)$$

(The expression for $\tilde{V}_H^{a\text{c}}(r)$ differs from that of Ref. 28 because here we assume $\tilde{n}_{\text{core}}^a(r) \equiv 0$.) For evaluating both the reference Hartree potential and reference pseudoexchange kernel function

$$\tilde{X}_v(r) \Big|_{\text{ref}} = - \sum_{v'} \sum_{L=|l_v-l_{v'}|}^{l_v+l_{v'}} \frac{1}{N_v} \Theta_{vv'}^L \tilde{W}_{v'v}^L(r) \Big|_{\text{ref}} \tilde{\psi}_{v'}(r), \quad (49)$$

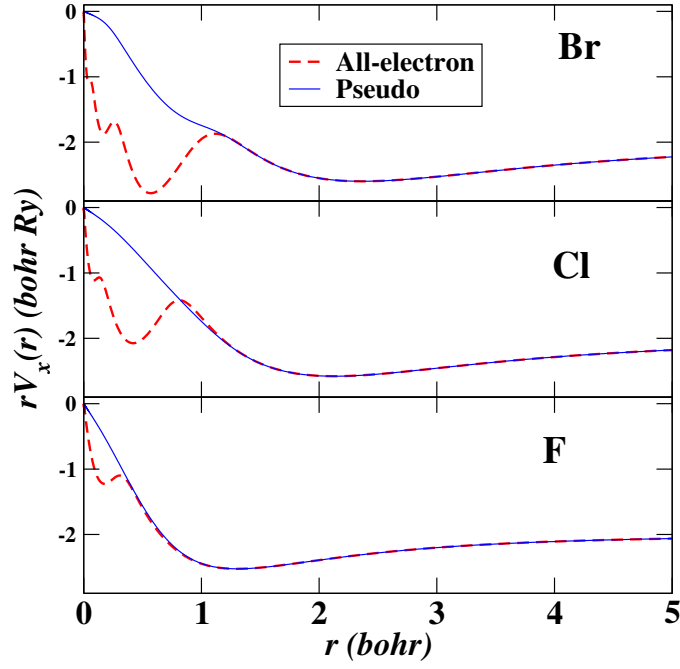


FIG. 5. (Color on line) Comparison of KLI all-electron ($V_x(r)$) and pseudo ($\tilde{V}_x(r)$) local exchange potentials for Br, Cl, and F in their ground states.

the interaction function can be evaluated from

$$\left[\tilde{W}_{v'v}^L(r) \right]_{\text{ref}} = e^2 \int_0^\infty dr' \frac{r'^L}{r_{>}^{L+1}} \left[\tilde{\psi}_{v'}(r') \tilde{\psi}_v(r') + \widehat{M}_{v'v}^L(r') \right], \quad (50)$$

For the reference configuration, the shell labels v' and v correspond to valence basis functions so that the moment functions have the simplified form

$$\left[\widehat{M}_{v'v}^L(r) \right]_{\text{ref}} = g_L(r) \int_0^{r_c^a} dr' r'^L \left[\psi_{v'}(r') \psi_v(r') - \tilde{\psi}_{v'}(r') \tilde{\psi}_v(r') \right]. \quad (51)$$

Figure 5 shows the pseudo versions of the KLI local exchange potentials given in Fig. 3. Figure 6 shows some examples of the unscreened local pseudopotential, $\tilde{V}_{\text{loc}}^a(r)$, showing that for the same choices of construction parameters the shapes are quite similar to those of LDA. These results for F,⁴⁶ Cl,⁴⁷ and Br,⁴⁸ were generated using a variation of the *atom paw* code²⁹, using the Vanderbilt⁴⁹ scheme for generating the pseudo basis and projector functions.

III. PLANE WAVE REPRESENTATIONS OF PAW-HF AND PAW-KLI EQUATIONS

In order to develop the projector augmented wave approach for Hartree-Fock and KLI formalisms to treat periodic systems, it is necessary to extend the equations presented in Ref. 28 and in Sec. II C to consider multiple atomic sites a and additional angular dependence. A pseudo wavefunction for Bloch state of band n and wavevector \mathbf{k} , can be represented in a plane wave expansion of the form

$$\tilde{\Psi}_{n\mathbf{k}}(\mathbf{r}) = \sqrt{\frac{1}{\mathcal{V}}} \sum_{\mathbf{G}} A_{n\mathbf{k}}(\mathbf{G}) e^{i(\mathbf{k}+\mathbf{G}) \cdot \mathbf{r}}, \quad (52)$$

where \mathcal{V} denotes the unit cell volume, $A_{n\mathbf{k}}(\mathbf{G})$ is an expansion coefficient, and the summation over reciprocal lattice vectors \mathbf{G} includes all terms for which $|\mathbf{k} + \mathbf{G}|^2 \leq E_{\text{cut}}$, for an appropriate cutoff parameter E_{cut} . For simplicity, we assume a spin unpolarized system with band weight and occupancy factors $f_{n\mathbf{k}}$.

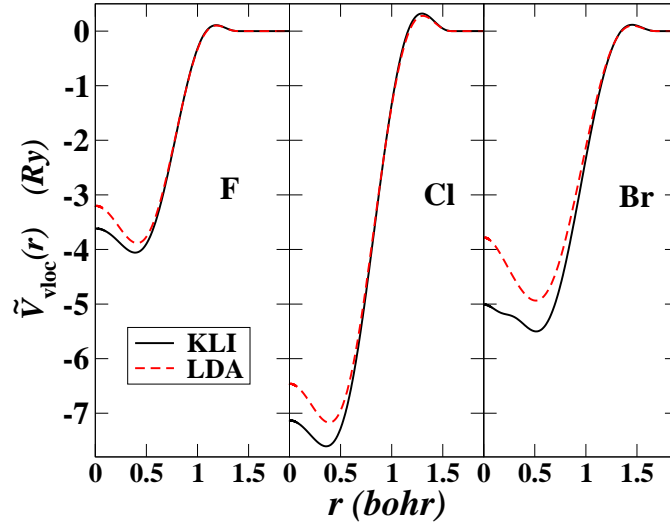


FIG. 6. (Color on line) Plots of $\tilde{V}_{\text{loc}}^a(r)$ for F, Cl, and Br, comparing KLI results with the corresponding LDA results.

A. Total energy expressions

The formulas for the total valence energy are the same in both the Hartree-Fock and KLI treatments. The energy differences are only due to differences in the wavefunctions used to evaluate the energies. Here we focus on the the Fock exchange term only, since the other contributions are identical to those found earlier papers.^{38,50–52} The total valence exchange energy is a sum of smooth and one-center contributions of the form

$$E_x|_{\text{val}} = \tilde{E}_x^{vv} + \sum_a \left(E_x^{avv} + E_x^{avc} - \tilde{E}_x^{avv} \right). \quad (53)$$

The fact that the core-valence interactions enter only in the one-center all-electron term is a consequence of our assumption that upper core states are treated as valence electrons so that only core states localized within the augmentation sphere are treated as frozen core states.

1. Smooth contributions to the Fock energy

For the purposes of evaluating the Fock energy and interaction terms, the smooth pair density function for band indices $n\mathbf{k}$ and $n'\mathbf{k}'$ can be written

$$\tilde{\rho}_{n\mathbf{k},n'\mathbf{k}'}(\mathbf{r}) \equiv \tilde{\Psi}_{n\mathbf{k}}(\mathbf{r})\tilde{\Psi}_{n'\mathbf{k}'}^*(\mathbf{r}) + \hat{\rho}_{n\mathbf{k},n'\mathbf{k}'}(\mathbf{r}), \quad (54)$$

where the second terms is the compensation pair charge.^{4,28} For a non-spherical system, the forms of these moments must be generalized from those presented in Eq. (58) of Ref. 28, in the form:⁵³

$$\hat{\rho}_{n\mathbf{k},n'\mathbf{k}'}(\mathbf{r}) = \sum_{aij} \langle P_i^a | \tilde{\Psi}_{n\mathbf{k}} \rangle \langle \tilde{\Psi}_{n'\mathbf{k}'} | P_j^a \rangle \hat{\mu}_{ij}^a(\mathbf{r} - \mathbf{R}^a), \quad (55)$$

where the generalized moments are given by

$$\hat{\mu}_{ij}^a(\mathbf{r}) \equiv \sum_{LM} \frac{G_{l_j m_j l_i m_i}^{LM}}{\sqrt{4\pi}} \frac{\hat{m}_{ji}^{aL}(r)}{r^2} Y_{LM}(\hat{\mathbf{r}}). \quad (56)$$

Here all of the terms are the same as defined in Ref. 28 except for the Gaunt coefficient⁵⁴ which we take to be⁵⁵

$$G_{l_j m_j l_i m_i}^{LM} \equiv \sqrt{4\pi} \int d\Omega Y_{l_j m_j}^*(\hat{\mathbf{r}}) Y_{LM}^*(\hat{\mathbf{r}}) Y_{l_i m_i}(\hat{\mathbf{r}}). \quad (57)$$

By design, this pair density function has the property

$$\lim_{N \rightarrow \infty} \frac{1}{N} \int_{N\mathcal{V}} d^3r \tilde{\rho}_{n\mathbf{k},n'\mathbf{k}'}(\mathbf{r}) = \delta_{nn'} (2\pi)^3 \delta(\mathbf{k} - \mathbf{k}'). \quad (58)$$

The Fourier transform of the smooth pair density function, is defined to be

$$\bar{\rho}_{n\mathbf{k},n'\mathbf{k}'}(\mathbf{G}) \equiv \int_{\mathcal{V}} d^3r \left(\tilde{\rho}_{n\mathbf{k},n'\mathbf{k}'}(\mathbf{r}) e^{-i(\mathbf{k}-\mathbf{k}') \cdot \mathbf{r}} \right) e^{-i\mathbf{G} \cdot \mathbf{r}}. \quad (59)$$

The compensation pair charge contribution can be evaluated according to

$$\bar{\rho}_{n\mathbf{k},n'\mathbf{k}'}(\mathbf{G}) = \sum_{aij} \langle P_i^a | \tilde{\Psi}_{n\mathbf{k}} \rangle \langle \tilde{\Psi}_{n'\mathbf{k}'} | P_j^a \rangle \bar{\mu}_{ij}^a(\mathbf{k} - \mathbf{k}' + \mathbf{G}), \quad (60)$$

where

$$\begin{aligned} \bar{\mu}_{ij}^a(\mathbf{q}) &\equiv e^{-i\mathbf{q} \cdot \mathbf{R}^a} \sum_{LM} G_{l_j m_j l_i m_i}^{LM} \sqrt{4\pi} (-i)^L Y_{LM}(\hat{\mathbf{q}}) \\ &\times \int_0^{r_c^a} dr j_L(qr) \hat{m}_{ji}^{aL}(r), \end{aligned} \quad (61)$$

with $j_L(x)$ denoting a spherical Bessel function.

In terms of smooth pair densities, the corresponding Fock energy can be written in the form

$$\begin{aligned} \tilde{E}_x^{vv} &= -\frac{e^2}{4} \sum_{n\mathbf{k}n'\mathbf{k}'} f_{n\mathbf{k}} f_{n'\mathbf{k}'} \\ &\times \int d^3r d^3r' \frac{\tilde{\rho}_{n\mathbf{k},n'\mathbf{k}'}(\mathbf{r}) \tilde{\rho}_{n\mathbf{k},n'\mathbf{k}'}^*(\mathbf{r}')}{|\mathbf{r} - \mathbf{r}'|} \\ &= -\frac{e^2 \pi}{\mathcal{V}} \sum_{n\mathbf{k}n'\mathbf{k}'} f_{n\mathbf{k}} f_{n'\mathbf{k}'} \sum_{\mathbf{G}} \frac{|\tilde{\rho}_{n\mathbf{k},n'\mathbf{k}'}(\mathbf{G})|^2}{|\mathbf{k} - \mathbf{k}' + \mathbf{G}|^2}. \end{aligned} \quad (62)$$

The evaluation of this singular integral has been the subject of several investigations.^{56–60} In this work, we evaluated both the methods of Spencer and Alavi⁵⁷ and of Duchemin and Gygi⁵⁶ as described in more detail in a brief report.⁶¹ Results given in Sec. IV were obtained using the method of Spencer and Alavi.⁵⁷

2. One-center contributions to the Fock energy

The combinations of angular contributions that appear in the one-center Coulombic contributions, can be expressed in terms of the 4-index matrix elements

$$\mathcal{V}_{ij;kl}^a \equiv \sum_{LM} G_{l_i m_i l_j m_j}^{LM} (-1)^M G_{l_k m_k l_l m_l}^{L-M} \left(\frac{R_{ij;kl}^{aL} - \tilde{R}_{ij;kl}^{aL}}{2L+1} \right), \quad (63)$$

where the generalized Condon-Shortley radial interaction integrals $R_{ij;kl}^{aL}$ and $\tilde{R}_{ij;kl}^{aL}$ have been defined in Eqs. (63 and 64) of Ref. 28.

It is also convenient to define a weighted projector product

$$\mathbf{W}_{ij}^a \equiv \sum_{n\mathbf{k}} f_{n\mathbf{k}} \langle \tilde{\Psi}_{n\mathbf{k}} | P_i^a \rangle \langle P_j^a | \tilde{\Psi}_{n\mathbf{k}} \rangle. \quad (64)$$

In evaluating both $\mathcal{V}_{ij;kl}^a$ and \mathbf{W}_{ij}^a , each basis index i, j, k, l stands for both the radial and angular quantum numbers ($n_i l_i m_i$, etc.).

The one-center valence-valence contribution to the Fock energy can then be written as

$$E_x^{avv} - \tilde{E}_x^{avv} = -\frac{1}{4} \sum_{ijkl} \mathbf{W}_{il}^a \mathbf{W}_{kj}^a \mathcal{V}_{ij;kl}^a. \quad (65)$$

We note that in this formulation which follows Ref. 28 and is slightly different from that of our earlier work (Eqs. A26 and A31 of Ref. 50), the corresponding one-center Hartree energy contributions take the form

$$E_H^{avv} - \tilde{E}_H^{avv} = \frac{1}{2} \sum_{ijkl} \mathbf{W}_{ij}^a \mathbf{W}_{kl}^a \mathcal{V}_{ij;kl}^a. \quad (66)$$

The one-center valence-core contribution to the Fock energy depends only on the Condon-Shortley interaction integrals between valence all-electron basis functions and frozen-core orbitals and takes the form

$$E_x^{avc} = - \sum_{ij} \mathbf{W}_{ij}^a \delta_{l_i l_j} \delta_{m_i m_j} C_{ij}^a, \quad (67)$$

where

$$C_{ij}^a = \sum_{cL} \frac{N_c}{2} \begin{pmatrix} l_c & L & l_i \\ 0 & 0 & 0 \end{pmatrix}^2 R_{ic;cj}^{aL}. \quad (68)$$

Here the sum over c is a sum over core shells with occupancies $N_c = 2(2l_c + 1)$ for each atom a .

B. Fock exchange kernel for Hartree-Fock formalism

The generalization of Eqs. (70-74) of Ref. 28 for a Bloch state $n\mathbf{k}$ can be written

$$X_{n\mathbf{k}}^{\text{PAW}}(\mathbf{r}) = \tilde{X}_{n\mathbf{k}}^{\text{HF}}(\mathbf{r}) + \sum_{ai} |\tilde{P}_i^a\rangle X_{i,n\mathbf{k}}^a. \quad (69)$$

The pseudo-exchange kernel takes the form

$$\tilde{X}_{n\mathbf{k}}^{\text{HF}}(\mathbf{r}) = -\frac{1}{2} \sum_{n'\mathbf{k}'} f_{n'\mathbf{k}'} \tilde{W}_{n\mathbf{k},n'\mathbf{k}'}(\mathbf{r}) \tilde{\Psi}_{n'\mathbf{k}'}(\mathbf{r}), \quad (70)$$

where the interaction function is defined by

$$\begin{aligned} \tilde{W}_{n\mathbf{k},n'\mathbf{k}'}(\mathbf{r}) &\equiv e^2 \int d^3r' \frac{\tilde{\rho}_{n\mathbf{k},n'\mathbf{k}'}(\mathbf{r}')}{|\mathbf{r} - \mathbf{r}'|} \\ &= e^{i(\mathbf{k}-\mathbf{k}')\cdot\mathbf{r}} \sum_{\mathbf{G}} \widetilde{\tilde{W}}_{n\mathbf{k},n'\mathbf{k}'}(\mathbf{G}) e^{i\mathbf{G}\cdot\mathbf{r}}. \end{aligned} \quad (71)$$

The Fourier transform of the interaction kernel is given by

$$\widetilde{\tilde{W}}_{n\mathbf{k},n'\mathbf{k}'}(\mathbf{G}) = \frac{4\pi e^2}{\mathcal{V}} \frac{\tilde{\rho}_{n\mathbf{k},n'\mathbf{k}'}(\mathbf{G})}{|\mathbf{k} - \mathbf{k}' + \mathbf{G}|^2}. \quad (72)$$

In order to treat its singular behavior in evaluating the pseudo-exchange kernel and related quantities, we used the method of Spencer and Alavi⁵⁷ which was mentioned previously in the context of evaluating the smooth contributions to the exchange energy (Eq. (62)).

The one-center matrix elements for the Hartree-Fock pseudoexchange kernel function analogous to Eq. (73) in Ref. 28 (but simplified for treating only localized core orbitals) take the form

$$\begin{aligned} X_{i,n\mathbf{k}}^a &= -\frac{1}{2} \sum_{jkl} \langle \tilde{P}_l^a | \tilde{\Psi}_{n\mathbf{k}} \rangle \mathbf{W}_{kj}^a \mathcal{V}_{ij;kl}^a \\ &\quad - \frac{1}{2} \sum_{n'\mathbf{k}'} f_{n'\mathbf{k}'} \sum_j \langle \tilde{P}_j^a | \tilde{\Psi}_{n'\mathbf{k}'} \rangle Z_{n\mathbf{k},n'\mathbf{k}';ij}^a \\ &\quad - \sum_j \langle \tilde{P}_j^a | \tilde{\Psi}_{n\mathbf{k}} \rangle \delta_{l_i l_j} \delta_{m_i m_j} C_{ij}^a, \end{aligned} \quad (73)$$

where

$$\begin{aligned} Z_{n\mathbf{k},n'\mathbf{k}';ij}^a &\equiv \int d^3r \hat{\mu}_{ij}^a(\mathbf{r}) \tilde{W}_{n\mathbf{k},n'\mathbf{k}'}(\mathbf{r}) \\ &= \sum_{\mathbf{G}} \tilde{\mu}_{ij}^{a*}(\mathbf{k} - \mathbf{k}' + \mathbf{G}) \widetilde{\tilde{W}}_{n\mathbf{k},n'\mathbf{k}'}(\mathbf{G}). \end{aligned} \quad (74)$$

C. Fock exchange potential for KLI formalism

The smooth pseudoexchange kernel $\tilde{X}_{n\mathbf{k}}^{\text{KLI}}(\mathbf{r})$ in the KLI approximation analogous to Eq. (30) takes the same form as the Hartree-Fock expression given in Eq. (70), evaluated using the appropriate KLI pseudo wavefunctions $\tilde{\Psi}_{n\mathbf{k}}(\mathbf{r})$. The corresponding pseudo-space potential function $\tilde{V}_x^{\text{KLI}}(\mathbf{r})$ can be determined from an expression analogous to Eq. (21) in Sec. II C 2:

$$\tilde{V}_x^{\text{KLI}}(\mathbf{r}) = \frac{1}{\tilde{\rho}(\mathbf{r})} \left(\sum_{n\mathbf{k}} f_{n\mathbf{k}} \tilde{\Psi}_{n\mathbf{k}}^*(\mathbf{r}) \tilde{X}_{n\mathbf{k}}^{\text{KLI}}(\mathbf{r}) + \sum_{n\mathbf{k}} f_{n\mathbf{k}} |\tilde{\Psi}_{n\mathbf{k}}(\mathbf{r})|^2 (\bar{V}_{x\ n\mathbf{k}}^{\text{KLI}} - \bar{U}_{x\ n\mathbf{k}}^{\text{KLI}}) \right). \quad (75)$$

In this expression, the valence pseudo-density is given by

$$\tilde{\rho}(\mathbf{r}) \equiv \sum_{n\mathbf{k}} f_{n\mathbf{k}} |\tilde{\Psi}_{n\mathbf{k}}(\mathbf{r})|^2. \quad (76)$$

Once the constant matrix elements $\bar{V}_{x\ n\mathbf{k}}^{\text{KLI}}$ and $\bar{U}_{x\ n\mathbf{k}}^{\text{KLI}}$ are known, this expression can be evaluated most conveniently using fast fourier transform (FFT) methods.

The one-center contributions to the exchange kernel can also be derived by extension of the atomic formalism. The one-center all-electron full density for atom a can be written in the form

$$\rho^a(\mathbf{r}) = \sum_{ij} \mathbf{W}_{ij}^a \Phi_i^{a*}(\mathbf{r}) \Phi_j^a(\mathbf{r}) + \sum_c N_c \frac{|\psi_c^a(r)|^2}{4\pi r^2}, \quad (77)$$

where the first term represents the valence states spanned by PAW basis functions indices i and j , and the second term represents the localized core states with index c representing the core shells (with occupancy $N_c = 2(2l_c + 1)$) for that atom. In order to evaluate the summations involving the all-electron exchange kernel, it is convenient to define the following functions. Analogous to the first term on the right hand side of Eq. (22) we define

$$\sum_p N_p \psi_p^a(r) X_p^{\text{KLI}}(r) \rightarrow \Upsilon^{a\ cc}(r) + \Upsilon^{a\ cv}(\mathbf{r}) + \Upsilon^{a\ vv}(\mathbf{r}). \quad (78)$$

Representing pure core contributions, we define

$$\Upsilon^{a\ cc}(r) \equiv - \sum_{cc'} \sum_L \Theta_{cc'}^L W_{cc'}^{aL}(r) \frac{\psi_c^a(r) \psi_{c'}^a(r)}{4\pi r^2}, \quad (79)$$

using the all-electron notation introduced in Sec. II A. Representing mixed core-valence contributions, we define

$$\begin{aligned} \Upsilon^{a\ cv}(\mathbf{r}) &\equiv - \sum_{ijc} N_c \mathbf{W}_{ij}^a Y_{l_i m_i}^*(\hat{\mathbf{r}}) Y_{l_j m_j}(\hat{\mathbf{r}}) \frac{\phi_i^a(r) \psi_c^a(r)}{r^2} \\ &\times \sum_L \begin{pmatrix} l_j & L & l_c \\ 0 & 0 & 0 \end{pmatrix}^2 W_{jc}^{aL}(r). \end{aligned} \quad (80)$$

In order to represent the pure valence contributions it is convenient to define the following one-center functions for the all-electron states:

$$\Psi_{n\mathbf{k}}^a(\mathbf{r}) \equiv \sum_i \langle \tilde{P}_i^a | \tilde{\Psi}_{n\mathbf{k}} \rangle \Phi_i^a(\mathbf{r}). \quad (81)$$

and the pseudo states:

$$\tilde{\Psi}_{n\mathbf{k}}^a(\mathbf{r}) \equiv \sum_i \langle \tilde{P}_i^a | \tilde{\Psi}_{n\mathbf{k}} \rangle \tilde{\Phi}_i^a(\mathbf{r}). \quad (82)$$

The one-center all-electron pure valence contributions can be written in the form

$$\begin{aligned} \Upsilon^{a\ vv}(\mathbf{r}) &\equiv - \frac{1}{2} \sum_{ij; LM} \Phi_i^{a*}(\mathbf{r}) \Phi_j^a(\mathbf{r}) Y_{LM}^*(\hat{\mathbf{r}}) \\ &\times \left(\mathcal{W}_{LM}^{a\ ij}(r) + \left(\frac{r}{r_c^a} \right)^L \mathcal{B}_{LM}^{a\ ij} \right). \end{aligned} \quad (83)$$

The first term of this expression can be evaluate in terms of the interaction potentials (Eq. (33)) evaluated within the augmentation sphere

$$\Delta w_{kl}^{aL}(r) \equiv w_{kl}^{aL}(r) - \left(\frac{r}{r_c^a}\right)^L w_{kl}^{aL}(r_c^a) \quad (84)$$

with the expression

$$\mathcal{W}_{LM}^{a\ ij}(r) \equiv \sum_{kl} \mathbf{W}_{il}^a \mathbf{W}_{kj}^a \frac{\sqrt{4\pi}(-1)^M}{2L+1} G_{l_k m_k l_l m_l}^{L-M} \Delta w_{kl}^{aL}(r). \quad (85)$$

The second term of Eq. (83) is related to the boundary value constant $\omega_{v'v}^L$ defined in Sec. II C 2 and can be expressed in the form

$$\begin{aligned} \mathcal{B}_{LM}^{a\ ij} &\equiv \sum_{n\mathbf{k}} f_{n\mathbf{k}} \mathcal{B}_{LM\ n\mathbf{k}}^{a\ ij} \\ &\equiv \sum_{n\mathbf{k}} f_{n\mathbf{k}} \sum_{n'\mathbf{k}'} f_{n'\mathbf{k}'} \langle \tilde{\Psi}_{n\mathbf{k}} | \tilde{P}_i^a \rangle \langle \tilde{P}_j^a | \tilde{\Psi}_{n'\mathbf{k}'} \rangle \mathbf{J}_{n\mathbf{k},n'\mathbf{k}'}^{a\ LM}. \end{aligned} \quad (86)$$

Here the $\mathbf{J}_{n\mathbf{k},n'\mathbf{k}'}^{a\ LM}$ is the angular component of the pseudo interaction integral defined Eq. (71) expanded about the atomic site a and evaluated at the augmentation radius r_c^a :

$$\begin{aligned} \mathbf{J}_{n\mathbf{k},n'\mathbf{k}'}^{a\ LM} &= \\ &4\pi i^L \sum_{\mathbf{G}} \overline{\tilde{W}}_{n\mathbf{k},n'\mathbf{k}'}(\mathbf{G}) e^{i\mathbf{q}\mathbf{G} \cdot \mathbf{R}^a} Y_{LM}(\widehat{\mathbf{q}\mathbf{G}}) j_L(|\mathbf{q}\mathbf{G}|r_c^a). \end{aligned} \quad (87)$$

In this expression, $\mathbf{q}\mathbf{G} \equiv \mathbf{k} - \mathbf{k}' + \mathbf{G}$, \mathbf{R}^a denotes the atomic position, and $j_L(x)$ denotes the spherical Bessel function.

In terms of these functions, the one-center all-electron exchange potential function can be evaluated with the relation

$$\begin{aligned} V_x^{\text{KLI}}(\mathbf{r}) &= \frac{1}{\rho^a(\mathbf{r})} \left(\Upsilon^{a\ cc}(r) + \Upsilon^{a\ cv}(\mathbf{r}) + \Upsilon^{a\ vv}(\mathbf{r}) \right. \\ &\quad + \sum_{n\mathbf{k}} f_{n\mathbf{k}} |\Psi_{n\mathbf{k}}^a(\mathbf{r})|^2 (\bar{V}_{x\ n\mathbf{k}}^{\text{KLI}} - \bar{U}_{x\ n\mathbf{k}}^{\text{KLI}}) \\ &\quad \left. + \sum_c N_c \frac{|\psi_c^a(r)|^2}{4\pi r^2} (\bar{V}_{x\ c}^{\text{KLI}} - \bar{U}_{x\ c}^{\text{KLI}}) \right). \end{aligned} \quad (88)$$

The one-center pseudo density, by assumption includes only valence contributions and can be written in the form

$$\tilde{\rho}^a(\mathbf{r}) = \sum_{ij} \mathbf{W}_{ij}^a \tilde{\Phi}_i^{a*}(\mathbf{r}) \tilde{\Phi}_j^a(\mathbf{r}). \quad (89)$$

The one-center pseudo exchange function can be evaluated with an expression similar to that of Eq. (88):

$$\begin{aligned} \tilde{V}_x^{\text{aKLI}}(\mathbf{r}) &= \frac{1}{\tilde{\rho}^a(\mathbf{r})} \left(\tilde{\Upsilon}^{a\ vv}(\mathbf{r}) \right. \\ &\quad \left. + \sum_{n\mathbf{k}} f_{n\mathbf{k}} \left| \tilde{\Psi}_{n\mathbf{k}}^a(\mathbf{r}) \right|^2 (\bar{V}_{x\ n\mathbf{k}}^{\text{KLI}} - \bar{U}_{x\ n\mathbf{k}}^{\text{KLI}}) \right). \end{aligned} \quad (90)$$

The function $\tilde{\Upsilon}^{a\ vv}(\mathbf{r})$ is evaluated using an expression similar to Eq. (83), replacing the all-electron basis functions $\Phi_i^a(\mathbf{r})$ with pseudo basis functions $\tilde{\Phi}_i^a(\mathbf{r})$ and the all-electron basis function kernel $w_{kl}^{aL}(r)$ defined by Eq. (33) with the pseudo basis function kernel $\tilde{w}_{kl}^{aL}(r)$ defined by Eq. (37). By construction, the basis function kernels are equal at the augmentation radii r_c^a ; $w_{kl}^{aL}(r_c^a) = \tilde{w}_{kl}^{aL}(r_c^a)$, ensuring consistency of the equations.

In order to evaluate this expressions we need to determine the exchange integral matrix elements. Matrix elements corresponding to core shells, come only from the one-center terms:

$$\begin{aligned} \bar{U}_{x\ c}^{\text{KLI}} &= - \sum_{c';L} \frac{1}{N_c} \Theta_{cc'}^L R_{cc';c'c}^{aL} \\ &\quad - \frac{1}{2} \sum_{ij;L} \mathbf{W}_{ij}^a \delta_{l_i l_j} \delta_{m_i m_j} \begin{pmatrix} l_c & L & l_i \\ 0 & 0 & 0 \end{pmatrix}^2 R_{ic;cj}^{aL}. \end{aligned} \quad (91)$$

In practice, each distinct core shell implies a particular site label a and core-core contributions (c and c') are restricted to the same site. Matrix elements corresponding to the valence bands can be evaluated using the expression

$$\begin{aligned} \bar{U}_{x\mathbf{nk}}^{\text{KLI}} &= \int d^3r \tilde{\Psi}_{\mathbf{nk}}^*(\mathbf{r}) \tilde{X}_{\mathbf{nk}}^{\text{KLI}}(\mathbf{r}) \\ &\quad - \frac{1}{2} \sum_{a;ijkl} \langle \tilde{\Psi}_{\mathbf{nk}} | \tilde{P}_i^a \rangle \langle \tilde{P}_l^a | \tilde{\Psi}_{\mathbf{nk}} \rangle \mathbf{W}_{kj}^a \mathcal{U}_{ij;kl}^a \\ &\quad - \frac{1}{2} \sum_{a;ij;LM} \frac{G_{l_i m_i l_j m_j}^{LM}}{\sqrt{4\pi}} \frac{m_{ij}^{aL}}{(r_c^a)^L} \mathcal{B}_{LM}^{a\ ij} \\ &\quad - \sum_{a;ij} \langle \tilde{\Psi}_{\mathbf{nk}} | \tilde{P}_i^a \rangle \langle \tilde{P}_j^a | \tilde{\Psi}_{\mathbf{nk}} \rangle \delta_{l_i l_j} \delta_{m_i m_j} C_{ij}^a. \end{aligned} \quad (92)$$

In this expression, the coefficient $\mathcal{U}_{ij;kl}^a$ is similar to the one-center Coulomb coefficient $\mathcal{V}_{ij;kl}^a$ defined in Eq. (63) and is given by

$$\mathcal{U}_{ij;kl}^a \equiv \sum_{LM} G_{l_i m_i l_j m_j}^{LM} (-1)^M G_{l_k m_k l_l m_l}^{L-M} \frac{u_{ij;kl}^{aL}}{2L+1}, \quad (93)$$

where the radial Coulomb terms are defined according to

$$\begin{aligned} u_{ij;kl}^{aL} &\equiv \int_0^{r_c^a} dr \left(\phi_i^a(r) \phi_j^a(r) w_{kl}^{aL}(r) - \tilde{\phi}_i^a(r) \tilde{\phi}_j^a(r) \tilde{w}_{kl}^{aL}(r) \right) \\ &\quad - \frac{m_{ij}^{aL}}{(r_c^a)^L} w_{kl}^{aL}(r_c^a). \end{aligned} \quad (94)$$

As in the atomic formulation, in order to evaluate the three contributions to the exchange potential in Eqs. (75), (88), and (90), the potential matrix elements $\bar{V}_{x\mathbf{nk}}^{\text{KLI}}$ and $\bar{V}_{x\mathbf{c}}^{\text{KLI}}$ must first be determined by solving a set of linear equations. For this purpose, we define

$$\Xi_{\mathbf{nk}}^{\text{PAW}} \equiv \tilde{\Xi}_{\mathbf{nk}} + \sum_a \left(\Xi_{\mathbf{nk}}^a - \tilde{\Xi}_{\mathbf{nk}}^a \right), \quad (95)$$

where

$$\tilde{\Xi}_{\mathbf{nk}} \equiv \int d^3r \left| \tilde{\Psi}_{\mathbf{nk}}(\mathbf{r}) \right|^2 \frac{\sum_{n'\mathbf{k}'} f_{n'\mathbf{k}'} \tilde{\Psi}_{n'\mathbf{k}'}^*(\mathbf{r}) \tilde{X}_{n'\mathbf{k}'}^{\text{KLI}}(\mathbf{r})}{\tilde{\rho}(\mathbf{r})}, \quad (96)$$

and the one-center contributions can be written

$$\begin{aligned} \Xi_{\mathbf{nk}}^a - \tilde{\Xi}_{\mathbf{nk}}^a &\equiv \sum_{ij} \langle \tilde{\Psi}_{\mathbf{nk}} | \tilde{P}_i^a \rangle \langle \tilde{P}_j^a | \tilde{\Psi}_{\mathbf{nk}} \rangle \\ &\quad \times \left(\int_{r \leq r_c^a} d^3r \Phi_i^{a*}(\mathbf{r}) \Phi_j^a(\mathbf{r}) \frac{\Upsilon^{a\ cc}(r) + \Upsilon^{a\ cv}(\mathbf{r}) + \Upsilon^{a\ vv}(\mathbf{r})}{\rho^a(\mathbf{r})} \right. \\ &\quad \left. - \int_{r \leq r_c^a} d^3r \tilde{\Phi}_i^{a*}(\mathbf{r}) \tilde{\Phi}_j^a(\mathbf{r}) \frac{\tilde{\Upsilon}^{a\ vv}(\mathbf{r})}{\tilde{\rho}^a(\mathbf{r})} \right). \end{aligned} \quad (97)$$

The corresponding core shell contribution can be written

$$\Xi_c^{\text{PAW}} = \Xi_c^a, \quad (98)$$

where the notation implies that the core shell c corresponds to the particular atomic site a . The term may be evaluated with the expression

$$\Xi_c^a \equiv \int d^3r \frac{|\psi_c^a(r)|^2}{4\pi r^2} \frac{\Upsilon^{a\ cc}(r) + \Upsilon^{a\ cv}(\mathbf{r}) + \Upsilon^{a\ vv}(\mathbf{r})}{\rho^a(\mathbf{r})}. \quad (99)$$

The coupling matrix elements between valence states can be written in the form

$$\Gamma_{n\mathbf{k},n'\mathbf{k}'}^{\text{PAW}} = \tilde{\Gamma}_{n\mathbf{k},n'\mathbf{k}'} + \sum_a \left(\Gamma_{n\mathbf{k},n'\mathbf{k}'}^a - \tilde{\Gamma}_{n\mathbf{k},n'\mathbf{k}'}^a \right). \quad (100)$$

Here, the pseudo space contribution is given by

$$\tilde{\Gamma}_{n\mathbf{k},n'\mathbf{k}'} \equiv \int d^3r \frac{|\tilde{\Psi}_{n\mathbf{k}}(\mathbf{r})|^2 |\tilde{\Psi}_{n'\mathbf{k}'}(\mathbf{r})|^2}{\tilde{\rho}(\mathbf{r})}, \quad (101)$$

which can be evaluated using FFT techniques. The one-center contributions can be evaluated from the expressions

$$\begin{aligned} \Gamma_{n\mathbf{k},n'\mathbf{k}'}^a - \tilde{\Gamma}_{n\mathbf{k},n'\mathbf{k}'}^a = & \sum_{ijkl} \langle \tilde{\Psi}_{n\mathbf{k}} | \tilde{P}_i^a \rangle \langle \tilde{P}_j^a | \tilde{\Psi}_{n\mathbf{k}} \rangle \langle \tilde{\Psi}_{n'\mathbf{k}'} | \tilde{P}_k^a \rangle \langle \tilde{P}_l^a | \tilde{\Psi}_{n'\mathbf{k}'} \rangle \\ & \times \left(\int_{r \leq r_c^a} d^3r \frac{\Phi_i^{a*}(\mathbf{r}) \Phi_j^a(\mathbf{r}) \Phi_k^{a*}(\mathbf{r}) \Phi_l^a(\mathbf{r})}{\rho^a(\mathbf{r})} \right. \\ & \left. - \int_{r \leq r_c^a} d^3r \frac{\tilde{\Phi}_i^{a*}(\mathbf{r}) \tilde{\Phi}_j^a(\mathbf{r}) \tilde{\Phi}_k^{a*}(\mathbf{r}) \tilde{\Phi}_l^a(\mathbf{r})}{\tilde{\rho}^a(\mathbf{r})} \right). \end{aligned} \quad (102)$$

The coupling matrix elements between valence and core shells and between core shells have only one-center contributions and depend only on the particular atomic site a associated with that core shell.

$$\Gamma_{n\mathbf{k},c}^{\text{PAW}} = \Gamma_{n\mathbf{k},c}^a \quad \text{and} \quad \Gamma_{c,c'}^{\text{PAW}} = \Gamma_{c,c'}^a. \quad (103)$$

The one-center matrix elements are both Hermitian and can be evaluated from the expressions

$$\Gamma_{n\mathbf{k},c}^a = \sum_{ij} \langle \tilde{\Psi}_{n\mathbf{k}} | \tilde{P}_i^a \rangle \langle \tilde{P}_j^a | \tilde{\Psi}_{n\mathbf{k}} \rangle \int d^3r \frac{\Phi_i^{a*}(\mathbf{r}) \Phi_j^a(\mathbf{r})}{\rho^a(\mathbf{r})} \frac{|\psi_c^a(r)|^2}{4\pi r^2}, \quad (104)$$

and

$$\Gamma_{c,c'}^a = \int d^3r \frac{|\psi_c^a(r)|^2}{4\pi r^2} \frac{|\psi_{c'}^a(r)|^2}{4\pi r^2} \frac{1}{\rho^a(\mathbf{r})}. \quad (105)$$

For evaluating the one-center integrals, it is most convenient to use a procedure found efficient in previous work.⁵⁰ We use a generalized Gaussian quadrature method to sample the angular directions $\hat{\mathbf{r}}_\alpha$ with weight factors w_α with $\sum_\alpha w_\alpha = 4\pi$. For each direction, $\hat{\mathbf{r}}_\alpha$, (usually 144 points are sufficient) the radial integrals $0 \leq r \leq r_c^a$ are evaluated using usual finite-difference-based algorithms. For example

$$\begin{aligned} & \int d^3r \frac{\Phi_i^{a*}(\mathbf{r}) \Phi_j^a(\mathbf{r})}{\rho^a(\mathbf{r})} \frac{|\psi_c^a(r)|^2}{4\pi r^2} \\ & \approx \sum_\alpha w_\alpha Y_{l_i m_i}^*(\hat{\mathbf{r}}_\alpha) Y_{l_j m_j}(\hat{\mathbf{r}}_\alpha) \int_0^{r_c^a} dr \frac{\phi_i^a(r) \phi_j^a(r) |\psi_c^a(r)|^2}{4\pi r^2 \rho^a(r \hat{\mathbf{r}}_\alpha)}. \end{aligned} \quad (106)$$

The linear equations that must be solved can then be put in the form

$$\begin{aligned} & \sum_{n'\mathbf{k}'} (\delta_{n\mathbf{k},n'\mathbf{k}'} - \Gamma_{n\mathbf{k},n'\mathbf{k}'}^{\text{PAW}} f_{n'\mathbf{k}'}) \Delta_{n'\mathbf{k}'} \\ & - \sum_c \Gamma_{n\mathbf{k},c}^{\text{PAW}} N_c \Delta_c = \Xi_{n\mathbf{k}}^{\text{PAW}} - \bar{U}_{x n\mathbf{k}}^{\text{KLI}}, \end{aligned} \quad (107)$$

and

$$\begin{aligned} & \sum_{c'} (\delta_{c,c'} - \Gamma_{c,c'}^{\text{PAW}} N_{c'}) \Delta_{c'} \\ & - \sum_{n'\mathbf{k}'} \Gamma_{c,n'\mathbf{k}'}^{\text{PAW}} f_{n'\mathbf{k}'} \Delta_{n'\mathbf{k}'} = \Xi_c^{\text{PAW}} - \bar{U}_{x c}^{\text{KLI}}. \end{aligned} \quad (108)$$

TABLE II. PAW parameters used in calculations: the pseudopotential radius r_c^a (in bohr), list of shell designations $n_1 l_1(r_{m_1}) n_2 l_2(r_{m_2}) \dots$ of basis and projector functions used in the calculation and corresponding radii r_{m_i} (in bohr) used to match the all-electron and pseudo radial wavefunctions. The symbol ϵ indicates the use of unbound basis functions with energies (in Ry units) $\epsilon = (16.0, 10.0)$ and $(2.0, 2.0)$ for C and F respectively. In each case, the local potential was constructed using the Troullier-Martins scheme⁶² for a continuum wavefunction of energy $\epsilon = 0$ and $l = 2$.

Atom	r_c^a	$\{n_i l_i(r_{m_i})\}$
Li	1.6	$1s(1.4) 2s(1.6) 2p(1.6)$
C	1.3	$2s(1.3) \epsilon s(1.3) 2p(1.3) \epsilon p(1.3)$
F	1.5	$2s(1.5) \epsilon s(1.5) 2p(1.5) \epsilon p(1.5)$

In these expressions,

$$\Delta_{n\mathbf{k}} \equiv \bar{V}_{x n\mathbf{k}}^{\text{KLI}} - \bar{U}_{x n\mathbf{k}}^{\text{KLI}} \text{ and } \Delta_c \equiv \bar{V}_{x c}^{\text{KLI}} - \bar{U}_{x c}^{\text{KLI}}. \quad (109)$$

The dimension of the the coupling matrix $\mathbf{\Gamma}^{\text{PAW}}$ is equal to the number of occupied bands $n\mathbf{k}$ within the \mathbf{k} -point sampling grid and the number of core shells c for all of the atoms of the unit cell. As in the atomic case, the coupling matrix is rank deficient, but the linear Eqs. (107) and (108) can be solved up to an arbitrary constant potential shift. We chose to fix the potential constant by setting $\Delta_{n_0\mathbf{k}_0} = \Xi_{n_0\mathbf{k}_0}^{\text{PAW}} - \bar{U}_{x n_0\mathbf{k}_0}^{\text{KLI}}$, where the index $n_0\mathbf{k}_0$ corresponds to the highest Kohn-Sham eigenvalue associated with an occupied state.

Once the potential matrix elements $\bar{V}_{x n\mathbf{k}}^{\text{KLI}}$ and $\bar{V}_{x c}^{\text{KLI}}$ are determined, the corresponding exchange potentials can be calculated. While $\tilde{V}_x^{\text{KLI}}(\mathbf{r})$ (Eq. (75)) contributes to the Kohn-Sham pseudopotential evaluated over all space, the one center contributions given in Eqs. (88) and (90) contribute to the one-center matrix elements of the Hamiltonian D_{ij}^a in the form

$$[V_x^a]_{ij} \equiv \langle \Phi_i^a | V_x^{\text{aKLI}} | \Phi_j^a \rangle - \langle \tilde{\Phi}_i^a | \tilde{V}_x^{\text{aKLI}} | \tilde{\Phi}_j^a \rangle. \quad (110)$$

With the determination of these exchange potentials, the calculations proceed in the same way as other Kohn-Sham PAW algorithms.

IV. RESULTS FOR DIAMOND AND LiF

In order to test the formalism, we have calculated the self-consistent electronic structure of diamond and LiF. The PAW basis and projector functions were calculated using a modified version of the *atompaw* code²⁹ using the parameters listed in Table II. The same parameters were used to construct the Hartree-Fock, KLI, and LDA³⁶ datasets. While the results are not very sensitive to the details of the PAW parameters, past experience has shown that the choice of parameters given in Table II and a wavefunction plane-wave expansion cut-off of $|\mathbf{k} + \mathbf{G}|^2 \leq 64$ Ry are more than adequate to converge the calculations to benchmark values. Details of the Hartree-Fock dataset construction follow Ref. 28 and extensions described in Appendix B.

The solid calculations for the Hartree-Fock and KLI calculations were performed using a modified version of the *pwpaw* code.⁶³ The LDA results were obtained using the *abinit*⁶⁴ and *quantum-espresso*⁶⁵ codes as well. The Brillouin zone sampling was performed using a uniform $2 \times 2 \times 2$ grid. This sampling was found to be adequate for the LDA calculations; additional code development will be needed to substantially increase the Brillouin zone sampling for the Hartree-Fock and KLI portions of the code. The binding energy curves shown in Figs. 7 and 8 were fit to the Murnaghan equation of state⁶⁶ in order to extract the equilibrium lattice constant a and bulk modulus B which are reported in Table III. There are many results of these quantities in the literature; a few of these are listed for comparison in Table III, showing general consistency with the present results.

To the best of our knowledge, our PAW-HF formulation is similar if not identical to that of Paier and co-workers⁴ as implemented in the *VASP* code⁶⁷ and to that of the *GPaw* code¹² (apart from the replacement of the planewave expansion with a real space grid representation). In order to benefit from cancellation of systematic errors, we have been careful to use atomic PAW datasets (Table II) constructed with the same exchange-correlation or pure exchange formulation as used in the solid calculations. There is some discussion in the literature⁶⁸ that it is sometimes possible to use fixed atomic PAW datasets with the help of valence-core corrections to perform calculations with different exchange-correlation formulations. It is our experience that the choice of appropriate basis function sets and augmentation radii such as listed in Table II are rather insensitive to the exchange-correlation formulation. However, the basis and projector functions themselves as well as the local potential $\tilde{V}_{\text{loc}}^a(r)$ are more sensitive; these can easily be generated by using the *atompaw* code.²⁹

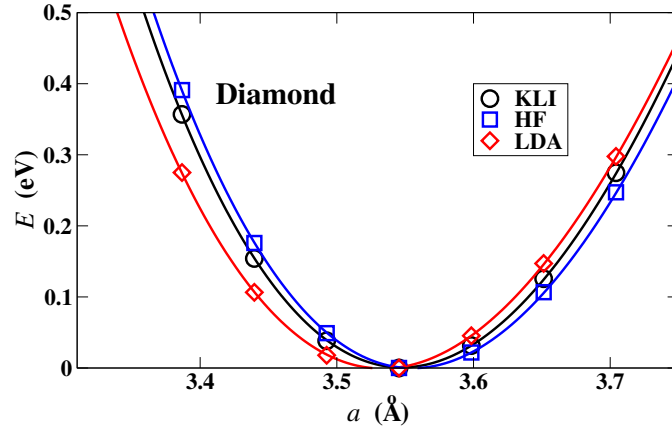


FIG. 7. (Color on line) Binding energy curve for C in the diamond structure.

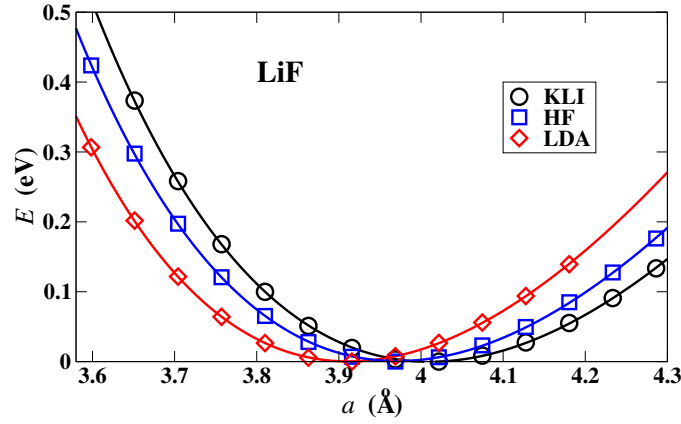


FIG. 8. (Color on line) Binding energy curve for LiF in the rock salt structure.

V. SUMMARY AND CONCLUSIONS

Using Fock exchange as an example of an orbital dependent functional, we have presented detailed equations needed to carry out self-consistent electronic structure calculations within the approximate optimized effective potential formalism developed by Krieger, Li, and Iafrate (KLI)³⁰ using the projector augmented wave method (PAW) of Blöchl.³⁸ This formalism together with the analogous development for the self-consistent Hartree-Fock formalism presented in earlier work²⁸ have been implemented and tested on the study of the ground state properties of two well-known crystalline materials – diamond and LiF. The fact that

TABLE III. Comparison of lattice parameters. Lattice constants a are given in Å and bulk moduli B are given in GPa.

	Diamond		LiF	
	a	B	a	B
LDA (this work)	3.53	490	3.91	85
LDA (literature)	3.54, ^a 3.55 ^b	452 ^b	3.92, ^a 3.96 ^b	83 ^b
HF (this work)	3.56	490	3.97	79
HF (literature)	3.58 ^b	480 ^b	4.02, ^b 4.01 ^c	76, ^b 79 ^c
KLI (this work)	3.55	460	4.01	76
Experiment	3.57 ^d	443 ^d	4.03 ^d	67 ^d

^a Ref. 69.

^b Ref. 70.

^c Ref. 71.

^d Ref. 72.

the present results are in general agreement with results reported in the literature using other computational methods, provides some measure of validation of our formalism. It is interesting and not unexpected that the Hartree-Fock and KLI results for the equilibrium lattice constants are increased relative to the LDA values and are closer to the experimental values.

Both Hartree-Fock and KLI methods have been previously implemented in all-electron and in norm-conserving pseudopotential codes by many authors, some of which we list here.^{59,60,73–78} However, the present work, as well as several other recent studies^{56,79–82} show that there continue to be non-trivial numerical challenges in the careful evaluation of the Fock exchange interaction. For the PAW method, the evaluation relies on the use of compensation pair charges (Eq. (55)) to ensure that all of the moments of charge are correctly represented in the exchange interactions terms. This extension of ideas presented in the original PAW formalism³⁸ was first introduced by Paier and co-workers.⁴ In principle, the correct treatment of the charge moments in PAW approach should have accuracy advantages over norm-conserving pseudopotential methods^{73,74,76,78,83,84} which explicitly control only the diagonal $L = 0$ pair charges. We also show that the treatment of core effects in the Fock exchange are best implemented in terms of frozen-core *orbitals* which can be accomplished with high accuracy within the PAW method. Whether this analysis of the numerical advantages of PAW over other pseudo-potential methods in the treatment of the Fock exchange interaction turn out to be numerically significant and/or computationally efficient, needs still to be quantified. Encouraging results have recently been reported by the *GPAW* developers¹² who evaluate the Fock exchange using the PAW method on a real-space grid.

Having introduced the detailed equations needed both for the Hartree-Fock and for the KLI implementations, we can begin to compare the numerical and physical approximations involved with both of them. While the complication of the equations presented in Sec. III C does appear to be daunting, we have demonstrated it to be manageable. In fact, the added complication of the KLI approach results in the determination of the local exchange potential $V_x^{\text{KLI}}(r)$ for use in Kohn-Sham equations. While much of interest in the “exact exchange” comes from improvements in the band gap energies,^{77,85} the few results presented in Sec. IV indicate that there are non-trivial effects on the structural properties as well. We expect to continue to compare the methods in future work.

There are several ways in which the present work can be extended. The equations here have assumed that the core states are localized within the augmentation spheres of each atom. This condition can be relaxed by introducing core pseudo-wavefunctions $\tilde{\psi}_c^a(r)$ as discussed in Ref. 28 and introducing corresponding modifications to the PAW-KLI equations. Another extension involves improving the KLI approximation by calculating the optimized effective potential within the subspace of occupied orbitals ($v^{\text{occ}}(\mathbf{r})$) as described by Bulat and Levy.³⁴ Operationally, this involves including some additional non-diagonal matrix elements of the local exchange potential and the exchange integral function in Eq. (10). In addition, we have discussed the possibility of extending the PAW methodology to treat the full OEP equations and have argued (see also Appendix A) that would require a significant increase in the number of PAW one-center basis functions. A similar experience was recently reported by Betzinger and co-workers⁷⁹ in the context of an accurate implementation of local exact exchange potentials with the full-potential linearized augmented-plane-wave method.

The scope of the present work goes beyond the accurate treatment of the Fock exchange interaction. By extension, the same techniques can be used to treat other orbital-dependent exchange-correlation functionals as they are being developed.

Appendix A: An example of orbital shift functions

Figure 9 shows an example of the shell contributions to the combined shift function (Eq. (9)) for atomic C in the spherically averaged $1s^2 2s^2 2p^2$ configuration. While each curve represents a complicated function, the sum of the curves is zero at all radii as required at convergence by Eq. (9).

Figure 10 shows the shape of the individual orbital shift functions $g_p(r)$ for atomic C which were determined from Eq. (5). While their magnitudes are small, their shapes are very complicated. From the forms of these functions it is evident that their accurate representation as a sum of atomic basis functions would require the use of a large number of basis functions. In particular, the PAW transformation Eq. (18) would require that in the augmentation region, both the all-electron valence orbital function $\psi_v(r)$ and the corresponding all-electron valence orbital shift function $g_v(r)$ be well represented by a sum of all-electron basis functions $\{\phi_i(r)\}$ for $r \leq r_c^a$:

$$\psi_v(r) \approx \sum_i \phi_i(r) \langle \tilde{P}_i^a | \tilde{\Psi}_v \rangle \text{ and } g_v(r) \approx \sum_i \phi_i(r) \langle \tilde{P}_i^a | \tilde{G}_v \rangle. \quad (\text{A1})$$

While the expansion of $\psi_v(r)$ is well-controlled, the expansion of $g_v(r)$ is computationally much more demanding. Without knowing the values of the expansion coefficients $\langle \tilde{P}_i^a | \tilde{G}_v \rangle$, the shape of the curves in Fig. 10 suggest that accurate representation of $g_v(r)$ requires many more terms than does accurate representation of $\psi_v(r)$. Our numerical tests³⁹ are consistent with this analysis. This would make a full PAW-OEP treatment much more computationally demanding than PAW-KLI.

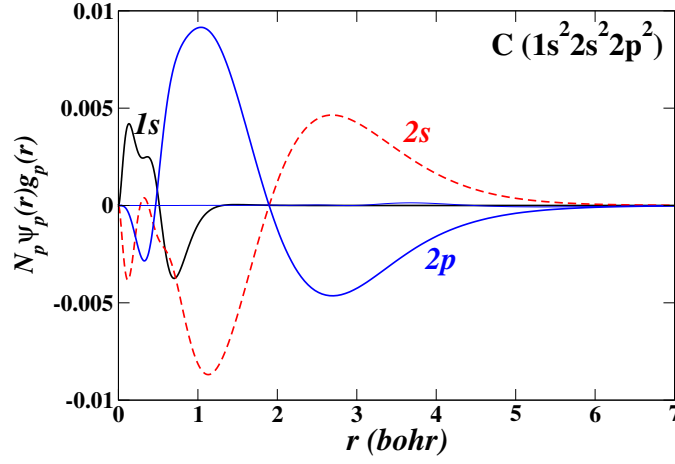


FIG. 9. (Color on line) Shell contributions to the combined shift function for C atom.

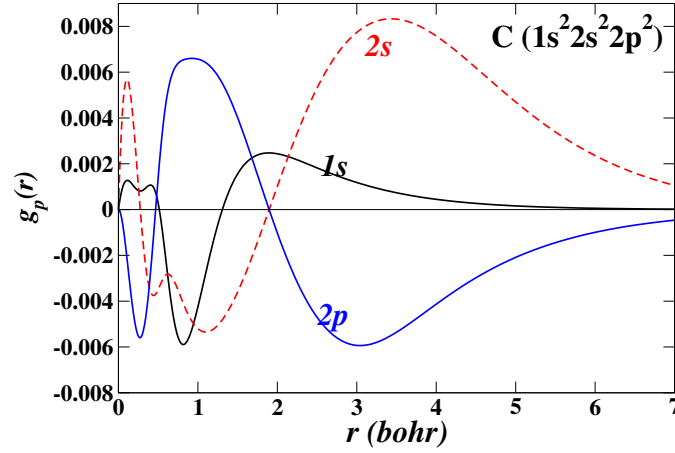


FIG. 10. (Color on line) Orbital shift functions $g_p(r)$ for C atom.

Appendix B: Some details of Hartree-Fock formalism

In principle, the Hartree-Fock equations are not defined for unoccupied states. However, in order to generate a more complete basis set for the PAW formalism and to generate $\tilde{V}_{\text{loc}}^a(r)$, it is convenient to use continuum states. For this purpose, we simplified a more rigorous treatment⁸⁶ and define a continuum state at a given energy $\epsilon_p > 0$ to satisfy the integral differential equation (similar to Eq. (17) of Ref. 28)

$$(\mathcal{K} + V_N(r) + V_H(r) - \epsilon_p) \psi_p(r) + X_p(r) = 0. \quad (\text{B1})$$

Here $X_p(r)$ is defined by Eq. (7) with the sum over q including only occupied states, and where no explicit orthonormalization constraints are imposed. In our previous work we noted that results can be sensitive not only to the basis functions, but also to the magnitude of the localized pseudopotential $\tilde{V}_{\text{loc}}^a(r)$. By using Eq. (B1) and a method similar to that described by Al-Saidi and co-workers⁸³ to generate a norm-conserving screened pseudopotential $V^{\text{aPS}}(r)$, we can then use a similar unscreening process described by Eq. (47) to determine a suitable $\tilde{V}_{\text{loc}}^a(r)$ for each atom.

In order to simplify the formulation of the Hartree-Fock PAW equations, we relaxed the orthogonality constraints of the valence wavefunctions with respect to the core orbitals. We also assumed the core states to be confined within the augmentation region using the expressions given in Sec. III A 1, III A 2, and III B.

Matrix elements of the Hartree-Fock equations in the Bloch basis are diagonal in wavevector \mathbf{k} and Hermitian with respect to band indices. In order to use the same diagonalization procedures that are used for the Kohn-Sham formulations, it is convenient

to regroup terms in the evaluation of matrix elements of the exchange interaction defined in Sec. III B:

$$\begin{aligned}\langle \tilde{\Psi}_{n''\mathbf{k}} | X_{n\mathbf{k}}^{\text{PAW}} \rangle &= \langle \tilde{\Psi}_{n\mathbf{k}} | X_{n''\mathbf{k}}^{\text{PAW}} \rangle^* \\ &\equiv \mathcal{X}_{n''n}^{1\mathbf{k}} + \sum_{ail} \langle \tilde{\Psi}_{n''\mathbf{k}} | \tilde{P}_i^a \rangle \mathcal{X}_{il}^2 \langle \tilde{P}_l^a | \tilde{\Psi}_{n\mathbf{k}} \rangle.\end{aligned}\quad (\text{B2})$$

Here

$$\mathcal{X}_{n''n}^{1\mathbf{k}} \equiv -\frac{2\pi e^2}{\mathcal{V}} \sum_{n'\mathbf{k}'} f_{n'\mathbf{k}'} \frac{\tilde{\rho}_{n''\mathbf{k},n'\mathbf{k}'}^*(\mathbf{G}) \tilde{\rho}_{n\mathbf{k},n'\mathbf{k}'}(\mathbf{G})}{|\mathbf{k} - \mathbf{k}' + \mathbf{G}|^2}, \quad (\text{B3})$$

and

$$\mathcal{X}_{il}^2 \equiv -\frac{1}{2} \sum_{jk} \mathbf{W}_{kj}^a \mathcal{V}_{ij;kl}^a - \delta_{l_i l_l} \delta_{m_i m_l} C_{il}^a. \quad (\text{B4})$$

The current version of the code was written with these equations. Further analysis will be needed to improve the efficiency of the calculations.

ACKNOWLEDGMENTS

This work was supported by NSF grants DMR-0427055 and DMR-0705239. Computations were performed on the Wake Forest University DEAC cluster, a centrally managed resource with support provided in part by the University. We would like to thank Alan Wright and Normand Modine of Sandia National Laboratory for their helpful advice and many discussions. We would also like to thank Akbar Salam, William C. Kerr, V. Paúl Pauca, and Freddie R. Salsbury Jr. for serving on the Ph. D. thesis committee.

* natalie@wfu.edu; <http://www.wfu.edu/~natalie>

¹ P. Hohenberg and W. Kohn, Physical Review **136**, B864 (1964).

² W. Kohn and L. J. Sham, Physical Review **140**, A1133 (1965).

³ M. Ernzerhof and G. E. Scuseria, J. Chem. Phys. **110**, 5029 (1999).

⁴ J. Paier, R. Hirschl, M. Marsman, and G. Kresse, J. Chem. Phys. **122**, 234102 (13pp) (2005).

⁵ P. Novák, J. Kuneš, L. Chaput, and W. E. Pickett, Phys. Stat. Sol.(b) **243**, 563 (2006).

⁶ F. Tran, P. Blaha, K. Schwarz, and P. Novák, Phys. Rev. B **74**, 155108/1 (2006).

⁷ X. Wu, E. J. Walter, A. M. Rappe, R. Car, and A. Selloni, Phys. Rev. B **80**, 115201 (5pp) (2009).

⁸ J. Paier, M. Marsman, K. Hummer, G. Kresse, I. C. Gerger, and J. G. Ángyán, J. Chem. Phys. **124**, 154709 (13pp) (2006).

⁹ J. Paier, B. G. Janesko, T. M. Henderson, G. E. Scuseria, A. Grüneis, and G. Kresse, J. Chem. Phys. **132**, 094103 (10pp) (2010).

¹⁰ A. Alkauskas, P. Broqvist, and A. Pasquarello, Physica Status Solidi B (2010).

¹¹ V. L. Chevrier, S. P. Ong, R. Armiento, M. K. Y. Chan, and G. Ceder, Phys. Rev. B **82**, 075122 (11pp) (2010).

¹² J. Enkovaara, C. Rostgaard, J. J. Mortensen, J. Chen, M. Dulak, L. Ferrighi, J. Gavnholt, C. Glinsvad, V. Haikola, H. A. Hansen, H. H. Kristoffersen, M. Kuusma, A. H. Larsen, L. Lehtovaara, M. Ljungberg, O. Lopez-Acevedo, P. G. M. J. Ojanen, T. Olsen, V. Petzold, N. A. Romero, J. Stausholm-Møller, M. Strange, G. A. Tritsarlis, M. Vanin, M. Walter, B. Hammer, H. Häkkinen, G. K. H. Madsen, R. M. Nieminen, J. K. Nørskov, M. Puska, T. T. Rantala, J. Schiøtz, K. S. Thygesen, and K. W. Jacobsen, Journal of Physics: Condensed Matter **22**, 253202 (24pp) (2010).

¹³ J. Harl and G. Kresse, Phys. Rev. B **77**, 045136 (8pp) (2008).

¹⁴ H.-V. Nguyen and S. de Gironcoli, Phys. Rev. B **79**, 205114 (12pp) (2009).

¹⁵ J. Harl and G. Kresse, Phys. Rev. Lett. **103**, 056401 (4pp) (2009).

¹⁶ A. Grüneis, M. Marsman, J. Harl, L. Schimka, and G. Kresse, J. Chem. Phys. **131**, 154115 (5pp) (2009).

¹⁷ H.-V. Nguyen and G. Galli, J. Chem. Phys. **132**, 044109 (8pp) (2010).

¹⁸ J. Harl, L. Schimka, and G. Kresse, Phys. Rev. B **81**, 115126 (18pp) (2010).

¹⁹ A. Heßelmann and A. Görling, Molecular Physics **108**, 359 (2010).

²⁰ S. Kümmel and L. Kronik, Rev. Mod. Phys. **80**, 3 (2008).

²¹ T. Grabo, T. Kreibich, S. Kurth, and E. K. U. Gross, in *Strong Coulomb Correlations in Electronic Structure Calculations: Beyond the local density approximation*, edited by V. I. Anisimov (Gordon and Breach Science Publishers, 2000) Chap. 4, pp. 203–311.

²² A. Görling, A. Ipatov, A. W. Götz, and A. Heßelmann, Z. Phys. Chem. **224**, 325 (2010).

²³ J. D. Talman, Computer Physics Communications **54**, 85 (1989).

²⁴ B. A. Shadwick, J. D. Talman, and M. R. Norman, Computer Physics Communications **54**, 95 (1989).

- ²⁵ C. F. Fischer, T. Brage, and P. Jönsson, *Computational Atomic Structure* (Institute of Physics Publishing, 1997) the associated computer code, the ATSP package, is available at the website <http://atoms.vuse.vanderbilt.edu/>.
- ²⁶ R. A. Hyman, M. D. Stiles, and A. Zangwill, *Phys. Rev. B* **62**, 15521 (2000).
- ²⁷ J. D. Talman, *Phys. Rev. A* **72**, 044502 (3pp) (2005).
- ²⁸ X. Xu and N. A. W. Holzwarth, *Phys. Rev. B* **81**, 245105 (14pp) (2010), <http://link.aps.org/doi/10.1103/PhysRevB.81.245105>.
- ²⁹ N. A. W. Holzwarth, A. R. Tackett, and G. E. Matthews, *Computer Physics Communications* **135**, 329 (2001), available from the website <http://pwpaw.wfu.edu>.
- ³⁰ J. B. Krieger, Y. Li, and G. J. Iafrate, *Phys. Rev. A* **45**, 101 (1992).
- ³¹ F. D. Sala and A. Görling, *J. Chem. Phys.* **115**, 5718 (2001).
- ³² M. Grüning, O. V. Gritsenko, and E. J. Baerends, *J. Chem. Phys.* **116**, 6435 (2002).
- ³³ V. N. Staroverov, G. E. Scuseria, and E. R. Davidson, *J. Chem. Phys.* **125**, 081104 (4pp) (2006).
- ³⁴ F. A. Bulat and M. Levy, *Phys. Rev. A* **80**, 052510 (7pp) (2009).
- ³⁵ J. P. Perdew, K. Burke, and M. Ernzerhof, *Phys. Rev. Lett.* **77**, 3865 (1996), erratum – *Phys. Rev. Lett.* **78**, 1396 (1997).
- ³⁶ J. P. Perdew and Y. Wang, *Phys. Rev. B* **45**, 13244 (1992).
- ³⁷ C. F. Fischer, *The Hartree-Fock method for atoms* (John Wiley & Sons, 1977).
- ³⁸ P. E. Blöchl, *Phys. Rev. B* **50**, 17953 (1994).
- ³⁹ X. Xu, *Orbital Dependent Functionals: An Atom Projector Augmented Wave Method Implementation*, Ph.D. thesis, Wake Forest University (2011).
- ⁴⁰ E. U. Condon and G. H. Shortley, *The Theory of Atomic Spectra* (Cambridge U. Press, 1967).
- ⁴¹ S. Kümmel and J. P. Perdew, *Phys. Rev. B* **68**, 035103 (2003).
- ⁴² S. Kümmel and J. P. Perdew, *Phys. Rev. Lett.* **90**, 043004 (2003).
- ⁴³ R. A. Lippert, N. A. Modine, and A. F. Wright, *J. Phys.: Condens. Matter* **18**, 4295 (2006).
- ⁴⁴ As shown in Ref. 34, there are many alternative derivations which lead to the KLI equations.
- ⁴⁵ As explained in our previous work (Ref. 28), we are using the core and valence labels c and v to refer to both the category label and the label for the individual states in each category.
- ⁴⁶ For F, the augmentation radius was $r_c^a = 1.4$ bohr. The basis functions were $2s$, ϵs , $2p$, and ϵp , with continuum energies 6 Ry and 4 Ry, respectively. The matching radii were 1.1 bohr for the valence states and 1.4 bohr for the continuum states.
- ⁴⁷ For Cl, the augmentation radius was $r_c^a = 1.6$ bohr. The basis functions were $2s$, $3s$, $2p$, and $3p$. All matching radii were 1.6 bohr.
- ⁴⁸ For Br, the augmentation radius was $r_c^a = 1.7$ bohr. The basis functions were $3s$, $4s$, $3p$, $4p$, $3d$, and ϵd with $\epsilon = 2$ Ry. All matching radii were 1.7 bohr except for the $3d$ state for which 1.2 bohr was used.
- ⁴⁹ D. Vanderbilt, *Phys. Rev. B* **41**, 7892 (1990), USPP code is available from the website <http://www.physics.rutgers.edu/~dhv/uspp/>.
- ⁵⁰ N. A. W. Holzwarth, G. E. Matthews, R. B. Dunning, A. R. Tackett, and Y. Zeng, *Phys. Rev. B* **55**, 2005 (1997).
- ⁵¹ G. Kresse and D. Joubert, *Phys. Rev. B* **59**, 1758 (1999).
- ⁵² M. Torrent, F. Jollet, F. Bottin, G. Zerah, and X. Gonze, *Computational Materials Science* **42**, 337 (2008).
- ⁵³ In this section, the basis function indices ($i, j \dots$) are used both as a short hand notation for the radial function index and for the composite indices including the spherical harmonic values $l_i m_i$. Hopefully the interpretation of the expressions will be clear from their context.
- ⁵⁴ J. A. Gaunt, *Phil. Trans. R. Soc. Lond. A* **228**, 151 (1929).
- ⁵⁵ Note that the factor of $\sqrt{4\pi}$ is included here for convenience, but is not present in the usual definition of Gaunt coefficients.
- ⁵⁶ I. Duchemin and F. Gygi, *Computer Physics Communications* **181**, 855 (2010).
- ⁵⁷ J. Spencer and A. Alavi, *Phys. Rev. B* **77**, 193110 (4pp) (2008).
- ⁵⁸ P. Carrier, S. Rohra, and A. Görling, *Phys. Rev. B* **75**, 205126 (10pp) (2007).
- ⁵⁹ S. Massidda, M. Posternak, and A. Baldereschi, *Phys. Rev. B* **48**, 5058 (1993).
- ⁶⁰ F. Gygi and A. Baldereschi, *Phys. Rev. B* **34**, 4405 (1986).
- ⁶¹ N. A. W. Holzwarth and X. Xu, Submitted for publication as a brief report.
- ⁶² N. Troullier and J. L. Martins, *Phys. Rev. B* **43**, 1993 (1991).
- ⁶³ A. R. Tackett, N. A. W. Holzwarth, and G. E. Matthews, *Computer Physics Communications* **135**, 348 (2001), available from the website <http://pwpaw.wfu.edu>.
- ⁶⁴ X. Gonze, B. Amadon, P. M. Anglade, J. M. Beuken, F. Bottin, P. Boulanger, F. Bruneval, D. Caliste, R. Caracas, M. Cote, T. Deutsch, L. Genovese, P. Ghosez, M. Giantomassi, S. Goedecker, D. R. Hamann, P. Hermet, F. Jollet, G. Jomard, S. Leroux, M. Mancini, S. Mazevet, M. J. T. Oliveira, G. Onida, Y. Pouillon, T. Rangel, G. M. Rignanese, D. Sangalli, R. Shaltaf, M. Torrent, M. J. Verstraete, G. Zerah, and J. W. Zwanziger, *Computer Physics Communications* **180**, 2582 (2009), code is available at the website <http://www.abinit.org>.
- ⁶⁵ P. Giannozzi, S. Baroni, N. Bonini, M. Calandra, R. Car, C. Cavazzoni, D. Ceresoli, G. L. Chiarotti, M. Cococcioni, I. Dabo, A. D. Corso, S. de Gironcoli, S. Fabris, G. Fratesi, R. Gebauer, U. Gerstmann, C. Gougousis, A. Kokalj, M. Lazzeri, L. Martin-Samos, N. Marzari, F. Mauri, R. Mazzarello, S. Paolini, A. Pasquarello, L. Paulatto, C. Sbraccia, S. Scandolo, G. Sclauzero, A. P. Seitsonen, A. Smogunov, P. Umari, and R. M. Wentzcovitch, *J. Phys.: Condens. Matter* **21**, 394402 (19pp) (2009), available from the website <http://www.quantum-espresso.org>.
- ⁶⁶ F. D. Murnaghan, *Proc. Nat. Acad. Sci. USA* **30**, 244 (1944).
- ⁶⁷ A non-public-domain code available from the Faculty of Physics, Universität Wien in Austria. Website: <http://cms.mpi.univie.ac.at/vasp/vasp/vasp.html>.
- ⁶⁸ A. E. Mattsson, R. Armiento, J. Paier, G. Kresse, J. M. Wills, and T. R. Mattsson, *J. Chem. Phys.* **128**, 084714 (11pp) (2008).
- ⁶⁹ P. Haas, F. Tran, and P. Blaha, *Phys. Rev. B* **79**, 085104 (10pp) (2009), erratum: *Phys. Rev. B* **79**, 209902(E) (2009).
- ⁷⁰ M. Causà and A. Zupan, *Chemical Physics Letters* **220**, 145 (1994).

- ⁷¹ K. Doll and H. Stoll, PRB **56**, 10121 (1997).
- ⁷² C. Kittel, *Introduction to Solid State Physics*, seventh ed. (John Wiley & Sons, 1996).
- ⁷³ D. M. Bylander and L. Kleinman, Phys. Rev. B **52**, 14566 (1995).
- ⁷⁴ D. M. Bylander and L. Kleinman, Phys. Rev. Lett. **74**, 3660 (1995).
- ⁷⁵ D. M. Bylander and L. Kleinman, International Journal of Modern Physics B **10**, 399 (1996).
- ⁷⁶ D. M. Bylander and L. Kleinman, Phys. Rev. B **54**, 7891 (1996).
- ⁷⁷ M. Städele, M. Moukara, J. A. Majewski, P. Vogl, and A. Görling, Phys. Rev. B **59**, 10031 (1999).
- ⁷⁸ E. Engel, A. Höck, R. N. Schmid, R. M. Dreizler, and N. Chetty, Phys. Rev. B **64**, 125111 (12pp) (2001).
- ⁷⁹ M. Betzinger, C. Friedrich, S. Blügel, and A. Görling, Phys. Rev. B **83**, 045105 (11pp) (2011).
- ⁸⁰ E. J. Bylaska, K. Tsemekhman, S. B. Baden, J. H. Weare, and H. Jonsson, Journal of Computational Chemistry **32**, 54 (2011).
- ⁸¹ X. Wu, A. Selloni, and R. Car, Phys. Rev. B **79**, 085102 (5pp) (2009).
- ⁸² P. Broqvist, A. Alkauskas, and A. Pasquarello, Phys. Rev. B **80**, 085114 (13pp) (2009).
- ⁸³ W. A. Al-Saidi, E. J. Walter, and A. M. Rappe, Phys. Rev. B **77**, 075112 (10pp) (2008).
- ⁸⁴ J. R. Trail and R. J. Needs, J. Chem. Phys. **122**, 014112 (11pp) (2005).
- ⁸⁵ S. Sharma, J. K. Dewhurst, and C. Ambrosch-Draxl, Phys. Rev. Lett. **95**, 136402 (2005).
- ⁸⁶ M. J. Seaton, Philosophical Transactions of the Royal Society of London. Series A. Mathematical and Physical Sciences **245**, 469 (1953).